Supplementary Information (SI) for Dalton Transactions.
This journal is © The Royal Society of Chemistry 2025

Supporting Information

Carbon–Carbon Bond Formation and Cleavage at Redox Active Bis(piridylimino)isoindole (BPI) Germylene Compounds

*Antonio I. Nicasio, Rosie J. Somerville, Pablo Sahagún, Enrique Soto, Joaquín López-Serrano and Jesús Campos.**

[a] *Departamento de Química Inorgánica and Centro de Innovación en Química Avanzada (ORFEO-CINQA), Instituto de Investigaciones Químicas (IIQ), Consejo Superior de Investigaciones Científicas (CSIC) and Universidad de Sevilla, 41092 Sevilla, Spain.*

*Corresponding author's e-mail address: jesus.campos@iiq.csic.es

Contents:

Experimental Procedures

General Information

All reactions and manipulations were carried out using standard Schlenk and glove-box techniques under an atmosphere of argon and of high purity nitrogen, respectively. All solvents were dried, stored over 4 Å molecular sieves, and degassed prior to use. Solution ^{1}H and ^{13}C NMR spectra were recorded on Bruker AVANCE NEO-300, AVANCE NEO-400, AVANCE III-400R and AVANCE NEO-500 spectrometers at 25 °C unless otherwise stated. Chemical shifts (δ) are expressed with a positive sign, in parts per million. ^{1}H and ^{13}C chemical shifts reported are referenced internally to residual solvent.[1] The following abbreviations and their combinations are used: br, broad; s, singlet; d, doublet; t, triplet; q, quartet; m, multiplet. The ^{1}H and ^{13}C resonance signals were assigned by means of 2D HSQC and HMBC experiments. For elemental analyses, a LECO TruSpec CHN analyser was utilized. Cyclic voltammetry measurements were performed with an Autolab potentiostat PGSTAT204 by Metrohm and an electrochemical cell inside a glovebox. A freshly polished glassy carbon working electrode by Metrohm, a counter electrode, and a Ag wire as (pseudo) reference electrode was used. As electrolyte $^{n}Bu_4NPF_6$ (0.1 M in THF) was used. Potentials were calibrated against the Fc/Fc^{+} couple by internal standardization with ferrocene. X-band EPR spectroscopy was performed on a Bruker EMX nano system standard VT spectrometer. $Ge[N(SiMe_3)_2]_2$,[2] ^{H}HBPI and ^{Me}HBPI ligands,[3] and potassium graphite (KC_8),[4] were prepared according to literature procedures. All other reagents were used as received from commercial suppliers.

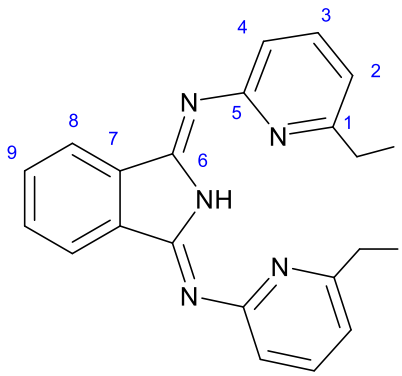

Synthesis of ^{Et}HBPI. The ligand was prepared following the general procedure reported for the preparation of 1,3-bis(2-pyridilimino)isoindoles.[3] A suspension of phthalonitrile (2.0 g, 15.6 mmol), 6-ethyl-2-aminopyridine (3.8 g, 31.22 mmol) and $CaCl_2$ (0.173 g, 1.56 mmol) in 1-hexanol (20 mL) was heated at reflux for 18 h. After this time, the mixture was cooled to room temperature and an orange solid precipitates. The solid was filtrated, washed with *n*-hexane and recrystallized in dichloromethane to obtain the ligand as orange crystals (yield: 4.72 g, 86%).

^{1}H NMR (400 MHz, $CDCl_3$, 25 °C) δ: 12.30 (br s, 1 H, NH), 8.06 (m, 2 H, H-8), 7.66 (d, 2 H, $^3J_{HH}$ = 8.1, H-4), 7.63 (d, 2 H, $^3J_{HH}$ = 7.3, H-9), 7.14 (d, 2 H, $^3J_{HH}$ = 7.7, H-2), 6.94 (d, 2 H, $^3J_{HH}$ = 7.5, H-3), 2.73 (q, 4 H, $^3J_{HH}$ = 7.6, –C*H*$_2$CH$_3$), 1.15 (t, 6 H, $^3J_{HH}$ = 7.6, –CH$_2$C*H*$_3$).

^{13}C{^{1}H} NMR (100 MHz, $CDCl_3$, 25 °C) δ: 162.5 (C-1), 160.3 (C-5), 153.1 (C-6), 138.6 (CH-4), 135.6 (C-7), 131.8 (CH-9), 122.7 (CH-8), 118.2 (CH-3), 118.1 (CH-2), 31.4 (–C*H*$_2$CH$_3$), 13.8 (–CH$_2$C*H*$_3$).

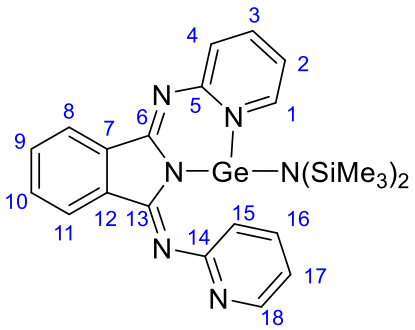

Synthesis of (κ²-*N*py,*N*iso-^{H}BPI)GeN(SiMe$_3$)$_2$ (1-H). To an orange solution of the ligand ^{H}HBPI (219 mg, 0.73 mmol) in toluene (6 mL) a solution of Ge[N(SiMe$_3$)$_2$]$_2$ (344 mg, 0.87 mmol) in toluene (4 mL) was added dropwise under argon atmosphere with vigorous stirring. After 30 minutes, volatiles were removed under vacuum. The remaining residue was precipitated and washed with pentane (3x3 mL) leading to a bright orange solid (yield: 260 mg, 67%).

Anal. Calcd. for $C_{24}H_{30}GeN_6Si_2$: C, 54.3; H, 5.7; N, 15.8. Found: C, 54.1; H, 5.9; N, 15.6.

^{1}H NMR (500 MHz, C_6D_6, 25 °C) δ: 8.36 (d, 1 H, $^{3}J_{HH}$ = 4.9, H-1), 8.08 (d, 1 H, $^{3}J_{HH}$ = 8.1, H-11), 8.06 (d, 1 H, $^{3}J_{HH}$ = 6.4, H-18), 7.27 (d, 1 H, $^{3}J_{HH}$ = 8.2, H-15), 7.17 (m, overlapped by solvent, 1 H, H-3), 7.10 (d, 1 H, $^{3}J_{HH}$ = 7.6, H-4), 7.09 (d, 1 H, $^{3}J_{HH}$ = 7.5, H-8), 6.98 (dd, 1 H, $^{3}J_{HH}$ = 8.1, 7.4, H-10), 6.88 (dd, 1 H, $^{3}J_{HH}$ = 8.2, 7.7, H-16), 6.81 (dd, 1 H, $^{3}J_{HH}$ = 7.5, 7.4, H-9), 6.58 (dd, 1 H, $^{3}J_{HH}$ = 7.2, 4.9, H-2), 6.25 (t, 1 H, $^{3}J_{HH}$ = 6.4, H-17), 0.33 (s, 18 H, Si-CH$_3$).

^{13}C{^{1}H} NMR (125 MHz, C_6D_6, 25 °C) δ: 161.6 (C, C-5), 161.0 (C, C-6), 160.7 (C, C-13), 157.9 (C, C-14), 149.1 (CH, C-1), 145.3 (CH, C-18), 141.1 (C, C-7), 140.8 (CH, C-16), 137.5 (CH, C-3), 131.4 (C, C-12), 131.3 (CH, C-9), 131.3 (CH, C-10), 125.9 (CH, C-8), 125.8 (CH, C-15), 123.0 (CH, C-11), 119.5 (CH, C-2), 119.2 (CH, C-17), 117.1 (CH, C-4), 5.5 (Si-CH$_3$).

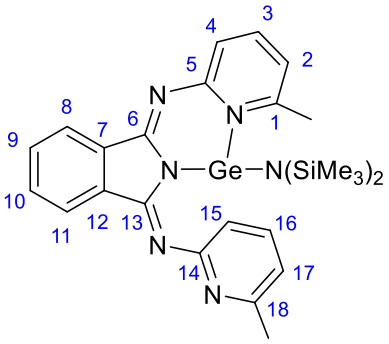

Synthesis of (κ^2-N_{py},N_{iso}-^{Me}BPI)GeN(SiMe$_3$)$_2$ (1-Me). Complex **1-Me** was prepared following the general procedure from Ge[N(SiMe$_3$)$_2$]$_2$ and ^{Me}HBPI (yield: 329 mg, 70%). Single-crystals of this compound suitable for X-Ray diffraction analysis were obtained from slow diffusion of pentane in saturated solutions of toluene.

Anal. Calcd. for $C_{26}H_{34}GeN_6Si_2$: C, 55.8; H, 6.1; N, 15.0. Found: C, 55.6; H, 6.5; N, 14.9.

^{1}H NMR (400 MHz, C_6D_6, 25 °C) δ: 8.08 (d, 1 H, $^3J_{HH}$ = 7.5, H-8), 7.27 (d, 1 H, $^3J_{HH}$ = 8.1, H-4), 7.18 (dd, 1 H, $^3J_{HH}$ = 7.5, 7.4, H-16), 7.04 (d, 1 H, $^3J_{HH}$ = 7.7, H-11), 7.00 (d, 1 H, $^3J_{HH}$ = 7.4, H-15), 6.98 (dd, 1 H, $^3J_{HH}$ = 8.3, 7.5, H-9), 6.87 (dd, 1 H, $^3J_{HH}$ = 8.1, 7.4, H-3), 6.82 (dd, 1 H, $^3J_{HH}$ = 8.3, 7.7 H-10), 6.57 (d, 1 H, $^3J_{HH}$ = 7.5, H-17), 6.09 (d, 1 H, $^3J_{HH}$ = 7.4, H-2), 2.70 (s, 3 H, CH$_3$-py), 2.38 (s, 3 H, CH$_3$-py'), 0.33 (s, 18 H, Si(CH$_3$)$_3$).

^{13}C{^{1}H} NMR (100 MHz, C_6D_6, 25 °C) δ: 160.8 (C, C-5), 160.3 (C, C-14), 158.3 (C, C-6), 158.3 (C, C-13), 157.7 (C, C-18), 156.0 (C, C-1), 140.6 (C, C-7), 139.8 (CH, C-3), 137.5 (CH, C-16), 131.4 (C, C-13), 130.8 (CH, C-9), 130.7 (CH, C-10), 125.3 (CH, C-11), 124.2 (CH, C-4), 122.6 (CH, C-8), 120.9 (CH, C-2), 118.2 (CH, C-17), 113.4 (CH, C-15), 24.1 (CH$_3$-py'), 22.8 (CH$_3$-py), 4.8 (Si(CH$_3$)$_3$).

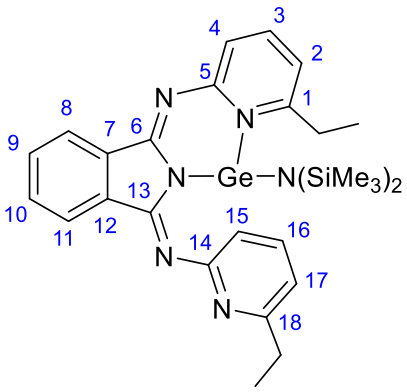

Synthesis of (κ^2-N_{py},N_{iso}-^{Et}BPI)GeN(SiMe$_3$)$_2$ (1-Et). Complex **1-Et** was prepared following the general procedure from Ge[N(SiMe$_3$)$_2$]$_2$ and ^{Et}HBPI (yield: 278 mg, 83%).

Anal. Calcd. for $C_{26}H_{34}GeN_6Si_2$: C, 57.3; H, 6.5; N, 14.3. Found: C, 57.1; H, 6.5; N, 14.5.

^{1}H NMR (500 MHz, C_6D_6, 25 °C) δ: 8.09 (dd, 1 H, $^3J_{HH}$ = 7.5, 1.0, H-8), 7.32 (dd, 1 H, $^3J_{HH}$ = 8.0, 1.3, H-4), 7.22 (t, 1 H, $^3J_{HH}$ = 7.5, H-16), 7.02 (d, 1 H, $^3J_{HH}$ = 7.5, H-15), 7.01, (d, 1 H, $^3J_{HH}$ = 7.5 H-11), 6.98 (dt, 1 H, $^3J_{HH}$ = 7.5, 1.0, H-9), 6.95 (dd, 1 H, $^3J_{HH}$ = 8.0, 7.7, H-3) 6.83 (td, 1 H, $^3J_{HH}$ = 7.5, 1.0, H-10), 6.60 (dd, 1 H, $^3J_{HH}$ = 7.5, 0.9, H-17), 6.26 (dd, 1 H, $^3J_{HH}$ = 7.7, 1.3, H-2), 3.45 (dq, 1 H, $^3J_{HH}$ = 15.0, 7.5, py-C*H*$_2$CH$_3$), 3.21 (dq, 1 H, $^3J_{HH}$ = 15.2, 7.5, py-C*H*$_2$CH$_3$), 2.69 (qd, 2 H, $^3J_{HH}$ = 7.6, 4.7, py'-C*H*$_2$CH$_3$), 1.24 (t, 3 H, $^3J_{HH}$ = 7.6, py'-CH$_2$C*H*$_3$), 1.12 (t, 3 H, $^3J_{HH}$ = 7.5, py-CH$_2$C*H*$_3$), 0.34 (s, 18 H, SiMe$_3$).

^{13}C{^{1}H} NMR (125 MHz, C_6D_6, 25 °C) δ: 163.1 (C, C-18), 161.7 (C, C-1), 161.2 (C, C-14), 160.7 (C, C-13), 158.4 (C, C-5), 158.4 (C, C-6), 141.0 (C, C-7), 140.4 (CH, C-3), 138.0 (CH, C-16), 131.8 (C, C-12), 131.2 (CH, C-9), 130.9 (CH, C-10), 125.7 (CH, C-11), 124.7 (CH, C-4), 122.9 (CH, C-8), 118.9 (CH, C-2), 117.6 (CH, C-17), 114.0 (CH, C-15), 31.7 (py'-*C*H$_2$CH$_3$), 28.8 (py-*C*H$_2$CH$_3$), 14.1 (py'-CH$_2$*C*H$_3$), 13.6 (py-CH$_2$*C*H$_3$), 5.1 (SiMe$_3$).

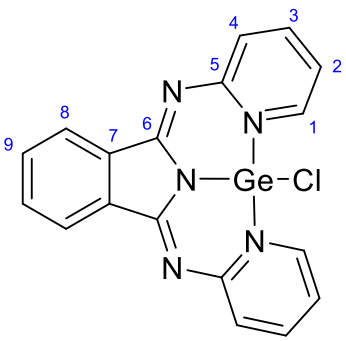

Synthesis of (κ^3-N_{py},N_{iso},N_{py}-^{H}BPI)GeCl (2-H). To a THF solution of the ligand ^{H}HBPI (233 mg, 0.78 mmol), a solution of K[N(SiMe$_3$)$_2$] (156 mg, 0.78 mmol) was added dropwise at –78ºC. The mixed solution was left to stir for 1 h during which it turned from a greenish solution to a bright yellow suspension. After this time, the product was twice washed with pentane (5 ml). Then, the solid was resuspended in THF and a solution of GeCl$_2$·dioxane (180 mg, 0.78 mmol) in THF was added leading to a change of colour from bright yellow to dark orange. The resulting product solution was dried under vacuum and washed with pentane (5 ml) twice, obtaining the desired complex as an orange solid (yield: 228 mg, 59%).

Anal. Calcd. for $C_{18}H_{12}ClGeN_5$: C, 53.2; H, 3.0; N, 17.2. Found: C, 53.5; H, 2.8; N, 16.9.

^{1}H NMR (500 MHz, THF-d$_8$, 25 °C) δ: 8.55 (dd, 2 H, $^{3}J_{HH}$ = 5.4, 1.9, H-1), 8.01 (dd, 2 H, *J* = 5.6, 3.1, H-8), 7.96 (td, 2 H, *J* = 7.7, 1.9, H-3), 7.62 (dd, 2 H, *J* = 5.6, 3.1, H-9), 7.54 (d, 2 H, $^{3}J_{HH}$ = 7.7, H-4), 7.30 (dd, 2 H, $^{3}J_{HH}$ = 7.7, 5.4, H-2).

^{13}C{^{1}H} NMR (125 MHz, THF-d$_8$, 25 °C) δ: 159.9 (C-6), 155.9 (C-5), 145.6 (CH-1), 141.9 (CH-3), 138.8 (C-7), 132.3 (CH-9), 125.8 (CH-4), 123.4 (CH-8), 121.4 (CH-2).

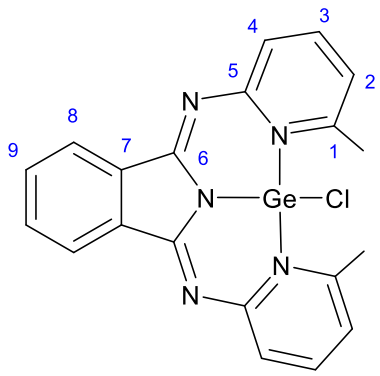

Synthesis of (κ^3-N_{py},N_{iso},N_{py}-^{Me}BPI)GeCl (2-Me). Complex **2-Me** was prepared following the general procedure from ^{Me}**HBPI** (yield: 236 mg, 70%).

Anal. Calcd. for $C_{20}H_{16}ClGeN_5$: C, 55.3; H, 3.7; N, 16.1. Found: C, 55.2; H, 3.5; N, 16.5.

^{1}H NMR (500 MHz, THF-d_8, 25 °C) δ: 7.98 (dd, 2 H, $^3J_{HH}$ = 5.5, 3.1, H-8), 7.77 (dd, 2 H, $^3J_{HH}$ = 8.0, 7.5, H-3), 7.61 (dd, 2 H, $^3J_{HH}$ = 5.5, 3.1, H-9), 7.35 (d, 2 H, $^3J_{HH}$ = 8.0, H-4), 7.00 (d, 2 H, $^3J_{HH}$ = 7.5, H-2), 2.85 (s, 6 H, CH_3-py).

^{13}C{^{1}H} NMR (125 MHz, THF-d_8, 25 °C) δ: 157.4 (C-1), 156.8 (C-6), 156.5 (C-5), 140.7 (CH-3), 138.7 (C-7), 132.2 (CH-9), 123.5 (CH-4), 123.4 (CH-8), 122.0 (CH-2), 21.8 (py-CH_3).

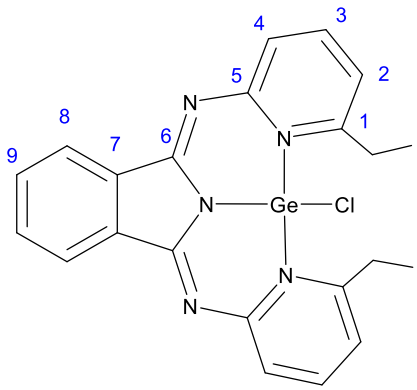

Synthesis of (κ^3-N_{py},N_{iso},N_{py}-^{Et}BPI)GeCl (2-Et). Complex **2-Et** was prepared following the general procedure from ^{Et}**HBPI** (yield: 260 mg, 72%).

Anal. Calcd. for $C_{22}H_{20}ClGeN_5$: C 57.1, H 4.3 N 15.1 Found: C 57.1, H 4.5, N 15.2.

^{1}H NMR (500 MHz, THF-d_8, 25 °C) δ: 8.00 (dd, 2 H, $^3J_{HH}$ = 5.6, 5.5, H-8), 7.83 (dd, 2 H, $^3J_{HH}$ = 8.0, 7.5, H-3), 7.63 (dd, 2 H, $^3J_{HH}$ = 5.6, 3.0, H-9), 7.37 (d, 2 H, $^3J_{HH}$ = 8.0, H-4), 7.07 (d, 2 H, $^3J_{HH}$ = 7.5, H-2), 3.25 (qd, 2 H, $^3J_{HH}$ = 14.8, 7.5, -C*H*$_2$CH$_3$), 3.20 (qd, 2 H, $^3J_{HH}$ = 14.8, 7.4, -C*H*$_2$CH$_3$), 1.37 (t, 6 H, $^3J_{HH}$ = 7.5, -CH$_2$C*H*$_3$).

^{13}C{^{1}H} NMR (125 MHz, THF-d_8, 25 °C) δ: 163.0 (C-1), 157.3 (C-5), 156.4 (C-6), 141.0 (CH-3), 138.7 (C-7), 132.3 (CH-9), 123.4 (CH-8), 123.3 (CH-4), 120.0 (CH-2), 29.0 (-*C*H$_2$CH$_3$), 14.7 (-CH$_2$*C*H$_3$).

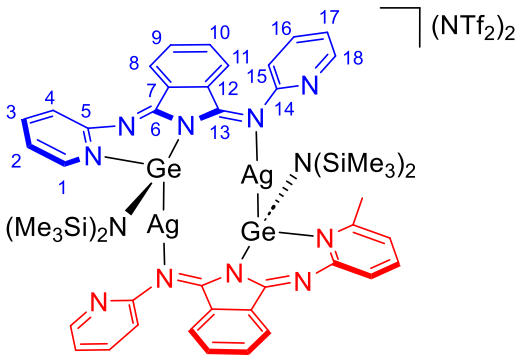

Synthesis of [{(HBPI)Ge(N(SiMe$_3$)$_2$)}(μ-Ag)$_2$]$_2$(NTf$_2$)$_2$ (3). To an orange solution of **1-H** (54 mg, 0.1 mmol) in toluene (3 mL) in a foil-wrapped vial was added a solution of silver bis(trifluoromethanesulfonate)amide (39 mg, 0.1 mmol) in toluene (2 mL) while stirring. After 5 minutes, 5 mL of diethyl ether were added and the resulting solution was placed in the freezer. The resulting yellow crystals were washed with pentane and dried under vacuum (yield: 79 mg, 86%). **Anal. Calcd.** for $C_{26}H_{30}AgF_6Ge_2N_7O_4S_2Si_4$: C, 34.0; H, 3.3; N, 10.7; S, 7.0. Found: C, 34.1; H, 3.2; N, 10.3; S, 6.7.

^{1}H NMR (500 MHz, $CDCl_3$, 25 °C) δ: 8.55 (m, 2 H, H-18), 8.20 (d, 2 H, $^3J_{HH}$ = 7.0, H-1), 8.18 (m, 2 H, H-3), 8.05 (td, 2 H, $^3J_{HH}$ = 7.5, 1.8, H-16), 7.73 (d, 2 H, $^3J_{HH}$ = 7.7, H-4), 7.69 (d, 2 H, $^3J_{HH}$ = 7.5, H-8), 7.57 (td, 2 H, $^3J_{HH}$ = 6.3, 1.4, H-2), 7.49 (t, 2 H, $^3J_{HH}$ = 5.0, H-9), 7.47 (t, 2 H, $^3J_{HH}$ = 5.2, H-17), 7.27 (m, 2 H, H-10), 7.24 (d, 2 H, $^3J_{HH}$ = 7.5, H-15), 6.63 (d, 2 H, $^3J_{HH}$ = 7.7, H-11), 0.06 (br, 18 H, Si-CH_3). **High-field region ^{1}H NMR** (400 MHz, $CDCl_3$, –20 °C) δ: 0.44 (s, 9 H, NSiMe$_3$), –0.37 (s, 9 H, NSiMe$_3$). **^{13}C{^{1}H} NMR** (100 MHz, $CDCl_3$, 25 °C) δ: 160.4 (C-13), 159.0 (C-14), 157.1 (C-6), 154.9 (C-5), 150.6 (CH-18), 145.8 (CH-1), 144.3 (CH-3), 141.9 (CH-16), 137.1 (C-12), 134.2 (CH-17), 133.7 (CH-15), 127.9 (CH-4), 127.0 (C-7), 125.8 (CH-11), 124.0 (CH-8), 123.4 (CH-2), 122.2 (CH-9), 117.9 (CH-10), 5.0 (Si-CH_3). **^{13}C{^{1}H} NMR** (100 MHz, $CDCl_3$, –20 °C) δ: 5.6 (Si-CH_3), 3.9 (Si-CH_3).

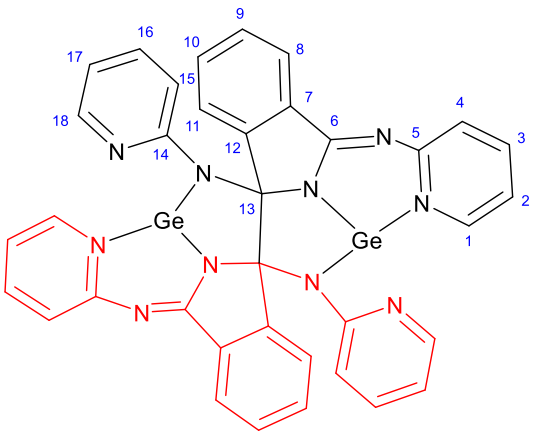

Synthesis of Ge_2(μ-κ^2-N_{py},N_{iso},κ^1-N_{imine}-^{H}BPI*) (4-H). Complex **2-H** (41 mg, 0.10 mmol) was weighed into a vial inside the glovebox and suspended in THF (3 ml). A suspension of KC_8 (14 mg, 0.10 mmol) in THF (2 ml) was added dropwise with vigorous stirring. After 30 min, during which the mixed solution turned from light orange to dark brown, the stirring was stopped and the THF solution was filtered into a clean vial, resulting in a clear orange solution. Finally, pentane (3 ml) was added to the vial and the mixture left to crystallise at –30 °C, obtaining the desired compound as reddish crystals (yield: 21 mg, 58%).

Anal. Calcd. for $C_{36}H_{24}Ge_2N_{10}$: C 58.3, H 3.3, N 18.9 Found: C 58.2, H 3.4, N 18.7.

^{1}H NMR (500 MHz, C_6D_6, 25 °C) δ: 8.78 (ddd, 2 H, $^3J_{HH}$ = 5.9, 2.0, 0.7, H-1,py), 7.99 (dt, 2 H, $^3J_{HH}$ = 7.6, 1.0, H-8), 7.96 (ddd, 2 H, $^3J_{HH}$ = 5.1, 2.0, 1.0, H-18,py'), 7.38 (dt, 2 H, $^3J_{HH}$ = 8.6, 1.3, H-4,py), 6.96 (ddd, 2 H, $^3J_{HH}$ = 8.6, 7.1, 2.0, H-3,py), 6.70 (m, 4 H, H-11 and H-16,py'), 6.67 (td, 2 H, $^3J_{HH}$ = 7.6, 1.0, H-9), 6.34 (td, 2 H, $^3J_{HH}$ = 7.6, 1.0, H-10), 6.27 (ddd, 2 H, $^3J_{HH}$ = 7.1, 5.9, 1.3, H-2,py), 6.24 (dt, 2 H, $^3J_{HH}$ = 8.5, 1.0, H-15,py'), 6.18 (ddd, 2 H, $^3J_{HH}$ = 7.1, 5.1, 1.0, H-17,py').

^{13}C{^{1}H} NMR (125 MHz, C_6D_6, 25 °C) δ: 161.1 (C-14), 160.7 (C-6), 158.6 (C-5), 146.9 (CH-18), 146.9 (CH-1), 145.3 (C-7), 139.8 (CH-3), 138.7 (C-12), 137.4 (CH-9), 130.4 (CH-10), 128.1 (overlapped by C_6D_6, CH-16), 125.0 (CH-4), 122.2 (CH-8), 122.0 (CH-11), 115.7 (CH-2), 113.1 (CH-17), 108.3 (CH-15), 94.6 (C, C-13).

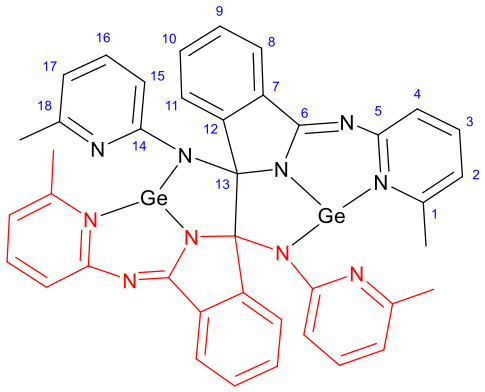

Synthesis of Ge_2(μ-κ^2-N_{py},N_{iso},κ^1-N_{imine}-^{Me}BPI*) (4-Me).

Complex **4-Me** was prepared following the general procedure from **2-Me** (yield: 24 mg, 62%).

Anal. Calcd. for $C_{40}H_{32}Ge_2N_{10}$·THF: C 60.7, H 4.6, N 16.1 Found: C 60.8, H 4.6, N 16.4.

^{1}H-NMR (500 MHz, C_6D_6, 25 °C) δ: 8.05 (d, 2 H, $^3J_{HH}$ = 7.5, H-8), 7.33 (d, 2 H, $^3J_{HH}$ = 8.2, H-4,py), 7.07 (d, 2 H, $^3J_{HH}$ = 7.6, H-11), 6.99 (dd, 2 H, $^3J_{HH}$ = 8.2, 7.3, H-3,py), 6.73 (dd, 2 H, $^3J_{HH}$ = 7.6, 7.5, H-9), 6.70 (dd, 2 H, $^3J_{HH}$ = 8.5, 7.2, H-16,py'), 6.50 (dd, 2 H, $^3J_{HH}$ = 7.6, 7.5, H-10), 6.17 (d, 2 H, $^3J_{HH}$ = 7.2, H-15,py'), 6.14 (d, 2 H, $^3J_{HH}$ = 7.3, H-2,py), 6.11 (d, 2 H, $^3J_{HH}$ = 8.5, H-17,py'), 2.83 (s, 6 H, CH_3-py), 2.20 (s, 6 H, CH_3-py').

^{13}C{^{1}H} NMR (125 MHz, C_6D_6, 25 °C) δ: 159.8 (C-14,py'), 159.6 (C-5,py), 159.1 (C-6), 155.8 (C-18,py'), 155.8 (C-1,py) 145.8 (C-6), 139.5 (CH-3,py), 138.5 (CH-12), 137.7 (CH-16,py'), 130.6 (CH-10), 128.5 (CH-9), 122.7 (CH-4,py), 122.6 (CH-8), 121.9 (CH-11), 117.8 (CH-2,py), 113.1 (CH-15,py'), 105.6 (CH-17,py'), 94.3 (C-13), 24.9 (CH_3-py), 23.3 (CH_3-py').

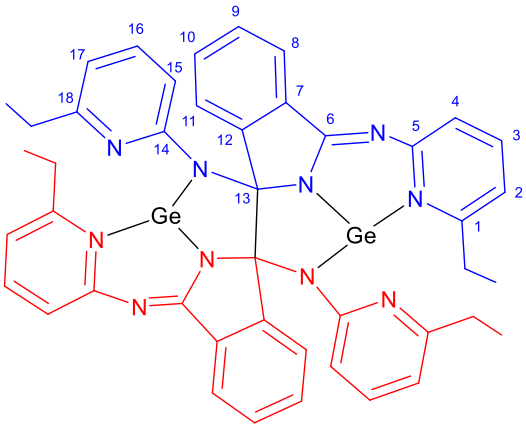

Synthesis of $Ge_2(\mu\text{-}\kappa^2\text{-}N_{py},N_{iso},\kappa^1\text{-}N_{imine}\text{-}{}^{Et}BPI^*)$ (5-Et).

Complex **5-Et** was prepared following the general procedure from **4-Et** (yield: 25 mg, 58%).

Anal. Calcd. for $C_{44}H_{40}Ge_2N_{10}\cdot THF$: C 62.2, H 5.2, N 15.1, Found: C 62.0, H 5.5, N 15.2.

^{1}H NMR (500 MHz, $CDCl_3$, 25 °C) δ: 7.72 (d, 2 H, $^3J_{HH}$ = 7.6, H-8), 7.68 (dd, 2 H, $^3J_{HH}$ = 8.2, 7.3, H-3), 7.17 (d, 2 H, $^3J_{HH}$ = 8.2, H-4), 7.10 (dd, 2 H, $^3J_{HH}$ = 7.6, 7.5, H-9), 7.01 (dd, 2 H, $^3J_{HH}$ = 8.4, 7.3, H-16), 6.95 (dd, 2 H, $^3J_{HH}$ = 7.6, 7.5, H-10), 6.86 (d, 2 H, $^3J_{HH}$ = 7.6, H-11), 6.82 (d, 2 H, $^3J_{HH}$ = 7.3, H-2), 6.41 (d, 2 H, $^3J_{HH}$ = 7.3, H-17), 5.64 (d, 2 H, $^3J_{HH}$ = 8.4, H-15), 3.37 (dq, 2 H, $^3J_{HH}$ = 14.9, 7.4, py-C*H*$_2$-CH$_3$), 3.29 (dq, 2 H, $^3J_{HH}$ = 15.0, 7.5, py-C*H*$_2$-CH$_3$), 2.66 (ddt, 4 H, $^3J_{HH}$ = 19.7, 14.9, 7.4, py-C*H*$_2$-CH$_3$), 1.27 (t, 6 H, $^3J_{HH}$ = 7.5, py-CH$_2$-C*H*$_3$), 1.00 (t, 6 H, $^3J_{HH}$ = 7.4, py-CH$_2$-C*H*$_3$).

^{13}C-NMR (125 MHz, $CDCl_3$, 25 °C) δ: 161.2 (C-1), 161.2 (C-18), 159.8 (C-5), 159.5 (C-14), 159.3 (C-6), 145.4 (C-7), 140.3 (C-3), 137.8 (C-16), 137.4 (C-12), 131.2 (C-10), 128.7 (C-10), 122.8 (C-8), 121.9 (C-4), 121.5 (C-11), 116.6 (C-2), 111.8 (C-17), 105.8 (C-15), 94.4 (C-13), 31.5 (py-*C*H$_2$CH$_3$), 30.8 (py-*C*H$_2$CH$_3$), 14.9 (py-CH$_2$*C*H$_3$), 13.7 (py-CH$_2$*C*H$_3$).

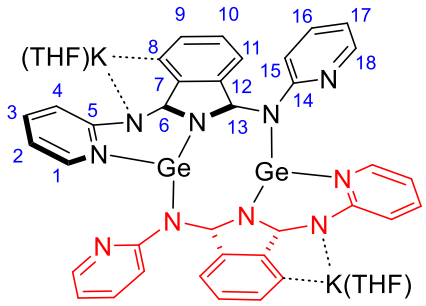

Synthesis of (μ-κ^2-N_{py},N_{iso},-κ^1-N_{imine}-^{H}BPI)Ge$_2$K$_2$·THF (5-H). To an orange solution of complex **2-H** (50 mg, 0.123 mmol) in THF (3 mL, –30 °C) was added KC_8 (33 mg, 0.246 mmol) in the glovebox with vigorous stirring. After 30 minutes, the resulting purple suspension was filtered and 3 mL of pentane was added slowly. The vial was placed in the glovebox freezer (–30 °C). After 2 days, dark-red crystals suitable for X-ray diffraction analysis were obtained (yield: 31 mg, 52%).

Anal. Calcd. for $C_{36}H_{24}Ge_2K_2N_{10}$·THF: C, 53.9; H, 3.5; N, 15.7. Found: C, 54.3; H, 3.7; N, 15.4.

^{1}H NMR (400 MHz, THF-d_8, 25 °C) δ: 7.89 (m, 4 H, H-1 and H-18), 7.13 (m, 2 H, H-8), 7.06 (ddd, 2 H, $^3J_{HH}$ = 8.8, 6.8, 2.1, H-3), 6.57 (m, 4 H, H-10 and H-16), 6.30 (dd, 2 H, $^3J_{HH}$ = 6.8, 5.1, H-2), 6.24 (d, 2 H, $^3J_{HH}$ = 8.8, H-4), 6.14 (dd, 4 H, $^3J_{HH}$ = 6.5, 3.0, H-11), 6.09 (d, 2 H, $^3J_{HH}$ = 9.0, H-15), 5.66 (td, 2 H, $^3J_{HH}$ = 6.3, 1.4, H-17), 3.58 (br, 4 H, THF), 1.73 (br, 4 H, THF).

^{13}C{^{1}H} NMR (100 MHz, THF-d_8, 25 °C) δ: 168.2 (C-5, py), 149.2 (C-14, py'), 147.5 (CH-1, py), 144.9 (CH-18, py'), 137.5 (CH-3, py), 132.3 (CH-16, py'), 128.2 (C-13), 124.7 (CH-15, py'), 123.7 (C-6), 120.4 (CH-8), 119.7 (CH-10), 118.4 (CH-9), 116.9 (C-7), 115.3 (CH-11), 115.1 (C-12), 111.9 (CH-2, py), 111.4 (CH-4, py), 104.2 (CH-17), 68.8 (CH, THF), 27.0 (CH, THF).

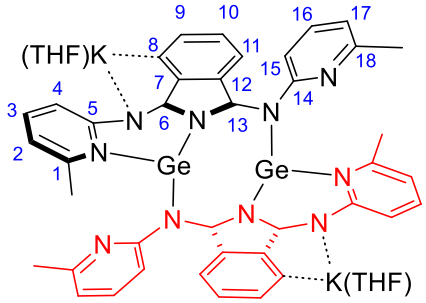

Synthesis of (μ-κ^2-*N*$_{py}$,*N*$_{iso}$,-κ^1-*N*$_{imine}$ -^{Me}BPI)Ge$_2$ (5-Me). Complex **5-Me** was prepared following the general procedure from **2-Me** (yield: 26 mg, 44%). **Anal. Calcd.** for $C_{40}H_{32}Ge_2K_2N_{10}$· 3 THF: C, 57.2, H, 5.1, N, 12.8. Found: C, 57.2, H, 5.0, N, 13.0. **^{1}H NMR** (500 MHz, THF-d$_8$, 25 °C) δ: 7.05 (d, 2 H, $^3J_{HH}$ = 8.3, H-8), 6.92 (dd, 2 H, $^3J_{HH}$ = 8.7, 7.0, H-3, py), 6.64 (d, 2 H, $^3J_{HH}$ = 8.5, H-11), 6.38 (dd, 2 H, $^3J_{HH}$ = 8.9, 6.2, H-16, py'), 6.14 (m, 4 H, H-2 and H-10), 6.07 (dd, 2 H, $^3J_{HH}$ = 8.3, 7.4, H-9), 5.93 (d, 4 H, $^3J_{HH}$ = 8.7, H-15, py'), 5.37 (d, 2 H, $^3J_{HH}$ = 6.2, H-17, py'), 3.53 (br, THF), 2.69 (s, 6 H, CH$_3$-py), 2.27 (s, 6 H, CH$_3$-py'), 1.67 (br, THF). **^{13}C{^{1}H} NMR** (125 MHz, THF-d$_8$, 25 °C) δ: 165.8 (C-5, py), 155.2 (C-14, py'), 152.1 (C-18, py'), 149.9 (C-13), 137.8 (CH-3, py), 131.2 (CH-16, py'), 127.3 (C-6), 123.1 (C-13), 122.9 (CH-15, py'), 119.8 (CH-8), 119.4 (CH-11), 117.6 (CH-10), 117.0 (C-12), 114.3 (CH-9), 114.0 (C-7), 110.5 (CH-2, py), 108.3 (CH-4, py), 104.9 (CH-17), 68.2 (THF), 26.4 (THF), 24.4 (CH$_3$-py), 24.1 (CH$_3$-py').

Crystal structure determinations

Low-temperature diffraction data were collected on a D8 Quest APEX-III single crystal diffractometer with a Photon III detector and a IμS 3.0 microfocus X-ray source. Data were collected by means of ω and φ scans using monochromatic radiation λ(Mo Kα1) = 0.71073 Å. The structures were solved with SHELXT and was refined against F^2 on all data by full-matrix least squares with SHELXL.[5] All non-hydrogen atoms were refined anisotropically. Hydrogen atoms were included in the model at geometrically calculated positions and refined using a riding model. In structures **2-H**, **4-H** and **5-Me**, the unit cells contain 1, 16 and 4 pentane molecules, respectively, which have been treated as a diffuse contribution to the overall scattering without specific atom positions by SQUEEZE/PLATON. Additional solvent molecules that could be precisely modelled were found in structures **3** (2 benzene molecules), **4-Me** (1 THF molecule), **4-Et** (1 THF molecule) and **5-H** (two free THF molecules and 4 additional THF molecules coordinated to the two independent potassium cations). Structure **2-Me** contains 2 independent molecules within asymmetric unit, while structure **3** was modelled as a twin with 75:25 components. A summary of the fundamental crystal and refinement data are given in Tables **S01-03**. Atomic coordinates, anisotropic displacement parameters and bond lengths and angles can be found in the cif files, which have been deposited in the Cambridge Crystallographic Data Centre with no. CCDC 2403134-2403143. These data can be obtained free of charge from The Cambridge Crystallographic Data Centre via www.ccdc.cam.ac.uk/data_request/cif

Table S01. Crystal data and structure refinement for compounds **1-H**, **2-H**, **2-Me** and **2-Et**.

	Compound **1-H**	Compound **2-H**	Compound **2-Me**	Compound **2-Et**
Formula	$C_{26}H_{34}GeN_6Si_2$	$C_{18}H_{12}ClGeN_5$	$C_{20}H_{16}ClGeN_5$	$C_{22}H_{20}ClGeN_5$
Fw	559.36	406.37	434.42	462.47
Crystal size (mm)	0.20 × 0.18 × 0.08	0.25 × 0.20 × 0.20	0.20 × 0.18 × 0.16	0.20 × 0.20 ×
Crystal system	Monoclinic	Tetragonal	Monoclinic	Triclinic
Space group	$P2_1/c$	$P4_3$	$P2_1/c$	$P\bar{1}$
a (Å)	11.1498 (3)	18.5687 (15)	16.5131 (8)	7.9741 (3)
b (Å)	29.6775 (9)	18.5687 (15)	13.2092 (8)	10.8973 (5)
c (Å)	8.7878 (2)	5.0359 (6)	16.4883 (9)	12.7245 (5)
α (º)	90	90	90	73.962 (2)
β (º)	103.037 (1)	90	98.056 (2)	73.763 (1)
γ (º)	90	90	90	78.458 (1)
V (Å^3)	2832.92 (13)	1736.4 (3)	3561.0 (3)	1011.21 (7)
T (K)	193	193	193	193
Z	4	4	8	2
ρ_{calc} (g·cm^{-3})	1.311	1.554	1.621	1.519
μ, mm^{-1} (MoKα)	1.19	1.93	1.89	1.67
F(000)	1168	816	1760	472
Absorption corrections	Multi-scan 0.640/0.746	Multi-scan 0.624/0.746	Multi-scan 0.618/0.746	Multi-scan 0.665/0.746
θ range (º)	2.0 – 27.5	2.2 – 28.3	2.4 – 27.2	2.8 – 28.7
Nº reflections measd	61649	15125	8840	36358
R_{int}	0.053	0.090	0.155	0.051
Nº reflections unique	5459	3371	6804	4186
Nº parameters/restraints	324 / 0	226 / 1	491 / 0	246 / 0
R_1 ($I > 2\sigma(I)$)[a]	0.042	0.073	0.132	0.037
R_1 (all data)	0.054	0.093	0.161	0.059
wR_2 (I > 2σ(I))	0.136	0.130	0.269	0.090
wR_2 (all data)	0.154	0.136	0.281	0.112
Diff. Fourier. peaks	-0.56 / 1.48	-0.76 / 1.02	-1.87 / 1.37	-0.63 / 0.92
CCDC number	2403136	2403143	2403137	2403134

Table S02. Crystal data and structure refinement for compounds **3**, **4-H** and **4-Me**.

	Compound **3**	Compound **4-H**	Compound **4-Me**
Formula	$C_{48}H_{60}Ag_2Ge_2N_{12}Si_4 \cdot 2(C_2F_6NO_4S_2) \cdot 2(C_6H_6)$	$C_{36}H_{24}Ge_2N_{10}$	$C_{44}H_{42}Ge_2N_{10}O$
Fw	1994.92	741.83	872.05
Crystal size (mm)	0.14 × 0.11 × 0.1	0.16 × 0.12 × 0.04	0.17 × 0.16 × 0.09
Crystal system	Triclinic	Monoclinic	Triclinic
Space group	$P\bar{1}$	$C2/c$	$P\bar{1}$
a (Å)	15.8097 (14)	21.1482 (17)	9.5726 (5)
b (Å)	16.6796 (15)	8.6859 (6)	12.0978 (6)
c (Å)	17.6314 (15)	22.075 (2)	17.3933 (10)
α (º)	99.488 (4)	90	91.942 (2)
β (º)	102.293 (4)	93.619 (3)	94.075 (2)
γ (º)	109.977 (4)	90	107.720 (2)
V (Å^3)	4124.1 (7)	4047.0 (6)	1910.58 (18)
T (K)	193	193	193
Z	2	4	2
ρ_{calc} (g·cm^{-3})	1.606	1.218	1.516
μ, mm^{-1} (MoKα)	1.44	1.52	1.63
F(000)	2008	1496	896
Absorption corrections	Multi-scan 0.574/0.745	Multi-scan 0.650/0.746	Multi-scan 0.642/0.746
θ range (º)	2.5 – 28.2	2.5 – 27.5	2.1 – 27.2
Nº reflections measd	20453	27806	66814
R_{int}	0.131	0.113	0.093
Nº reflections unique	20453	2859	6473
Nº parameters/restraints	992 / 36	218 / 0	516 / 2
R_1 ($I > 2\sigma(I)$)[a]	0.093	0.122	0.067
R_1 (all data)	0.167	0.143	0.089
wR_2 ($I > 2\sigma(I)$)	0.251	0.330	0.109
wR_2 (all data)	0.339	0.344	0.116
Diff. Fourier. peaks	-1.98 / 2.40	-1.59 / 1.87	-0.71 / 0.69
CCDC number	2403139	2403140	2403138

Table S03. Crystal data and structure refinement for compounds **4-Et**, **5-H** and **5-Me**.

	Compound **4-Et**	Compound **5-H**	Compound **5-Me**
Formula	$C_{48}H_{48}Ge_2N_{10}O$	$C_{60}H_{72}Ge_2K_2N_{10}O_6$	$C_{52}H_{55}Ge_2K_2N_{10}O_3$
Fw	926.14	1252.65	1091.44
Crystal size (mm)	0.24 × 0.23 × 0.18	0.08 × 0.07 × 0.04	0.11 × 0.10 × 0.04
Crystal system	Monoclinic	Triclinic	Monoclinic
Space group	*P*2/*n*	$P\bar{1}$	$P2_1/n$
a (Å)	13.3849 (5)	10.6413 (11)	14.1680 (5)
b (Å)	8.7408 (3)	15.2209 (19)	16.0363 (7)
c (Å)	18.0043 (6)	20.466 (2)	23.4696 (9)
α (º)	90	106.010 (5)	90
β (º)	95.169 (1)	99.137 (5)	94.698 (1)
γ (º)	90	95.273 (5)	90
V (Å^3)	2097.84 (13)	3113.5 (6)	5314.4 (4)
T (K)	193	193	193
Z	2	2	4
ρ_{calc} (g·cm^{-3})	1.466	1.336	1.364
μ, mm^{-1} (MoKα)	1.48	1.16	1.34
F(000)	956	1304	2252
Absorption corrections	Multi-scan 0.622/0.746	Multi-scan 0.478/0.746	Multi-scan 0.618/0.746
θ range (º)	2.3 – 29.1	2.0 – 25.3	1.9 – 27.1
Nº reflections measd	53015	95283	108974
R_{int}	0.049	0.232	0.125
Nº reflections unique	4589	6649	8243
Nº parameters/restraints	278 / 0	721 / 34	626 / 45
R_1 ($I > 2\sigma(I)$)[a]	0.040	0.085	0.048
R_1 (all data)	0.056	0.158	0.083
wR_2 ($I > 2\sigma(I)$)	0.099	0.179	0.134
wR_2 (all data)	0.109	0.223	0.165
Diff. Fourier. peaks	-0.44 / 0.84	-0.79 / 1.37	-0.87 / 0.54
CCDC number	2403135	2403141	2403142

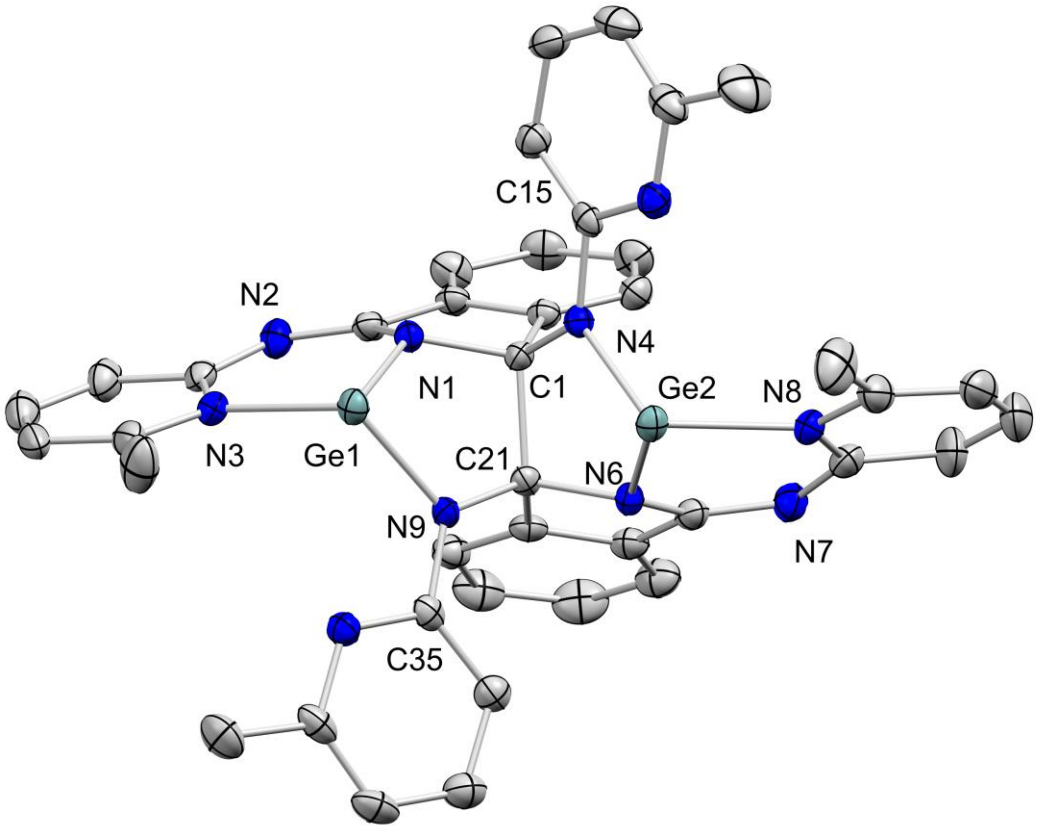

Figure S01. ORTEP of **4-Me** with 50% probability ellipsoids. Hydrogen atoms and solvent molecule (THF) are omitted for clarity.

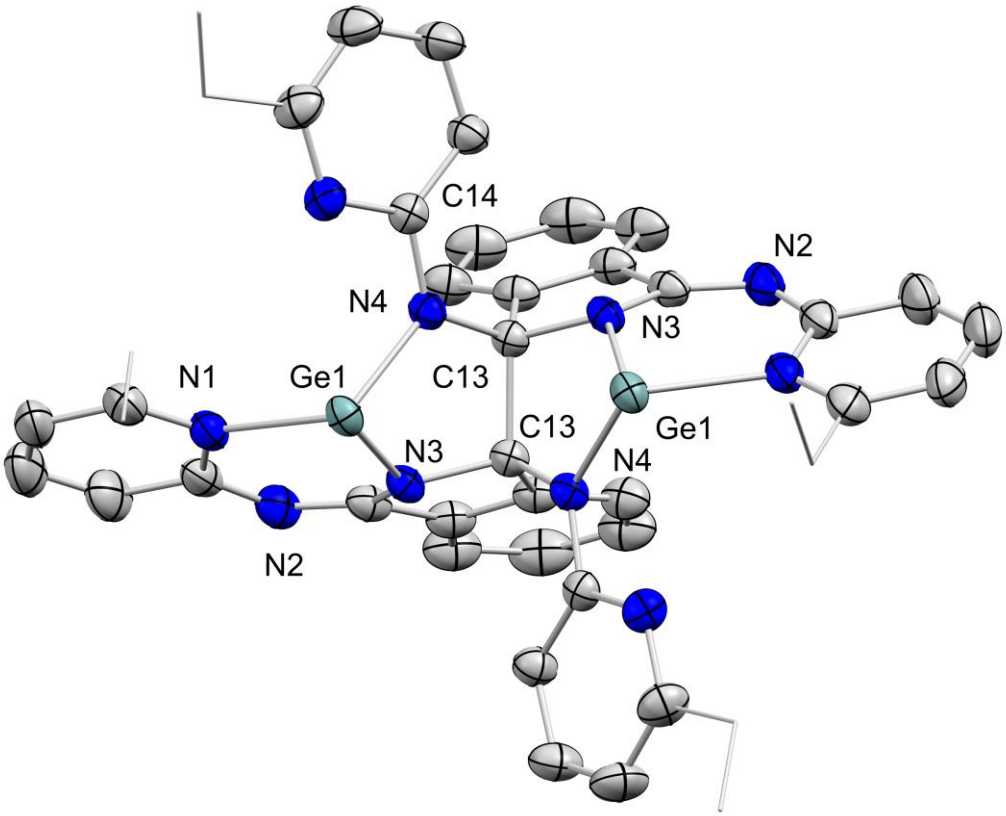

Figure S02. ORTEP of **4-Et**. For the sake of clarity, hydrogen atoms and solvent molecule (THF) are omitted and ethyl substituents are represented in wire-frame formal, while thermal ellipsoids are set at 50% probability.

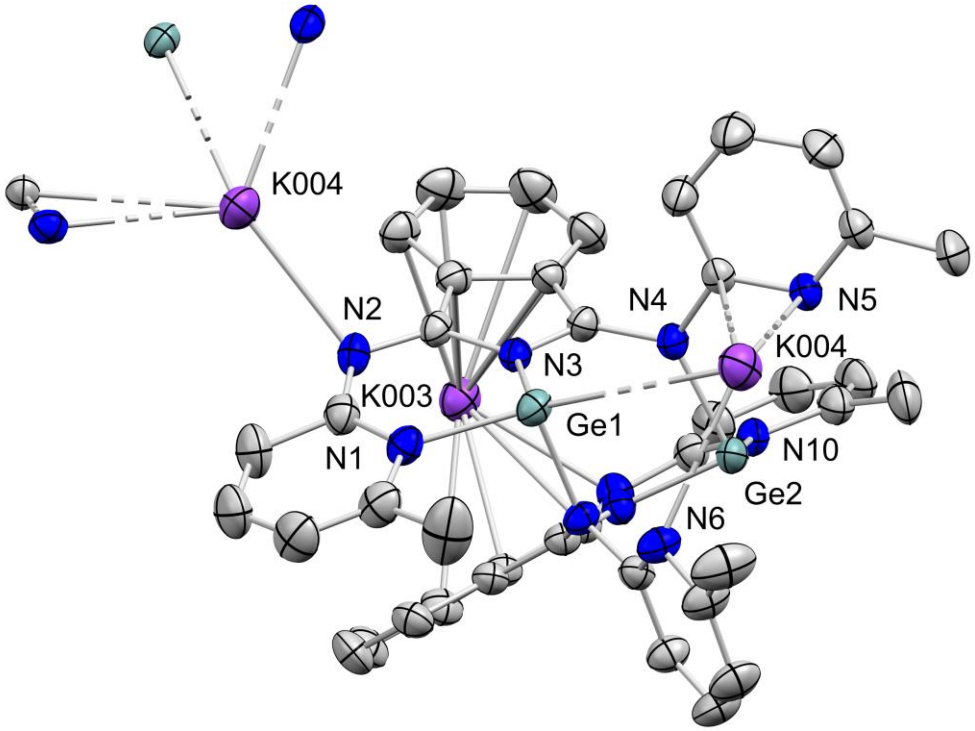

Figure S03. ORTEP of **5-Me** with 50% probability ellipsoids. Hydrogen atoms and solvent molecule (THF) are omitted for clarity.

Computational Details

Geometry optimizations were carried out without constraints with the Gaussian16 software[6] using the hybrid functional B3LYP[7,8] and the double-ζ basis set 6-31+g(d,p) with polarization and single diffuse functions for all atoms.[9–14] Dispersion effects were taken into account with the D3 version of Grimme's empirical dispersion with Becke-Johnson damping.[15,16] Bulk solvent effects (tetrahydrofurane) were considered at the optimization level with the SMD model.[17]

The optimized geometries were characterized as minima in the potential energy surface following vibrational analysis (no negative frequencies result from the analysis), which were also used to obtain the thermodynamic parameters, *G*, *H*, and *S*.

Final energies (E_{tz}) were obtained from single point calculations on previously optimized geometries at the same level of theory but replacing the double-ζ basis set by the triple-ζ quality basis set 6-311+(2d,p). Final free energies (G_{tz}) were calculated according to the following expression (1):

$$(1) \qquad G_{tz} = G_{dz} + (E_{tz} - E_{dz})$$

The internal stability of the wavefunction was checked for all calculations. Standard redox potentials were obtained from the calculated ΔG_{tz} values using the Nernst equation (2) and referenced to the calculated potential of the ferrocenium/ferrocene pair (3).[18]

$$(2) \quad E^{\circ} = -\frac{\Delta G^{\circ}}{nF}$$

$$(3) \quad Fc^{+} + \text{Reduced species} \rightleftharpoons Fc + \text{oxidized species}$$

Using this approach, our calculations of standard redox potentials underestimate the experimental values of the first reduction event for the species considered by an average of – 0.25 V. Thus, redox potentials were recalculated relative to the first reduction of the BPI ligand, using the experimental value of $E^{0}_{1/2,BPIH/BPIH^{-}}$ = – 2.06 V (vs Fc^{+}/Fc in THF) as a reference.[19]

Electron density plots were calculated with the Multiwfn program[20] from wavefunctions calculated at the triple-ζ level with Gaussian16. Some molecular geometries were generated with the Chemcraft program.[21]

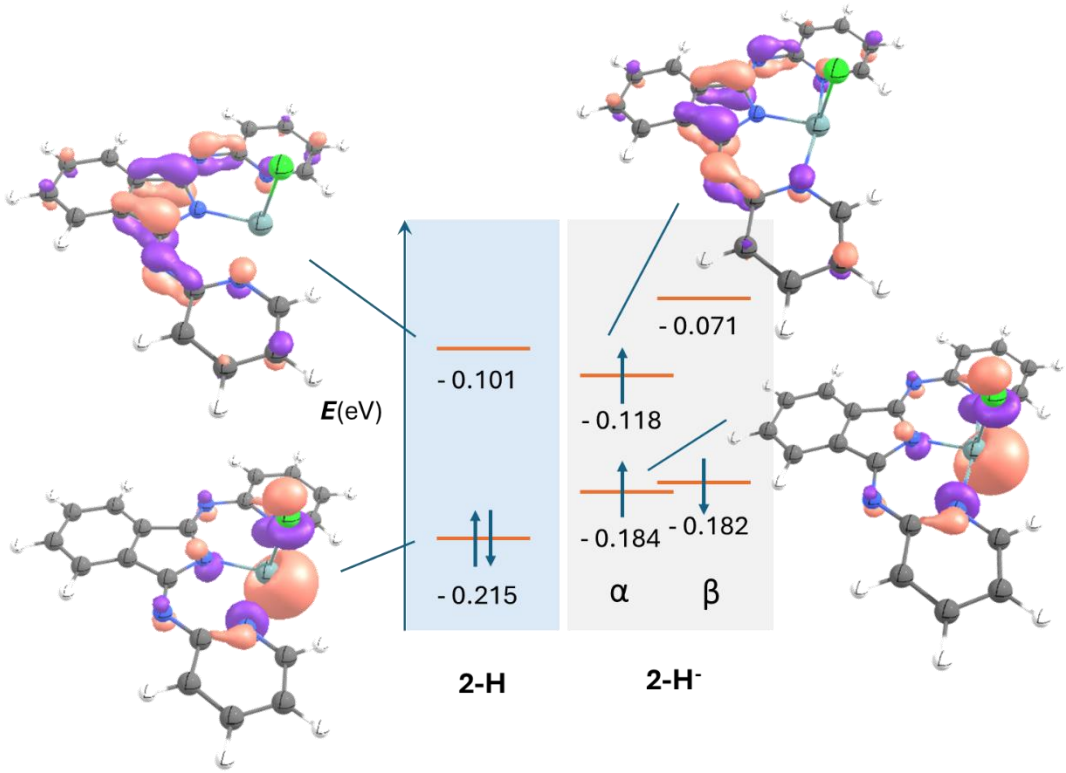

Figure S04. Frontier molecular orbitals of the neutral (left) and anionic (reduced; right) forms of **2-H**. The insets correspond to the HOMO and LUMO of **2-H** and the α-SOMO-1 and SOMO of **2-H**$^{-}$ at 0.06 a.u. isovalue. The spatial extension of the corresponding α and β MOs of **2-H**$^{-}$ is almost identical.

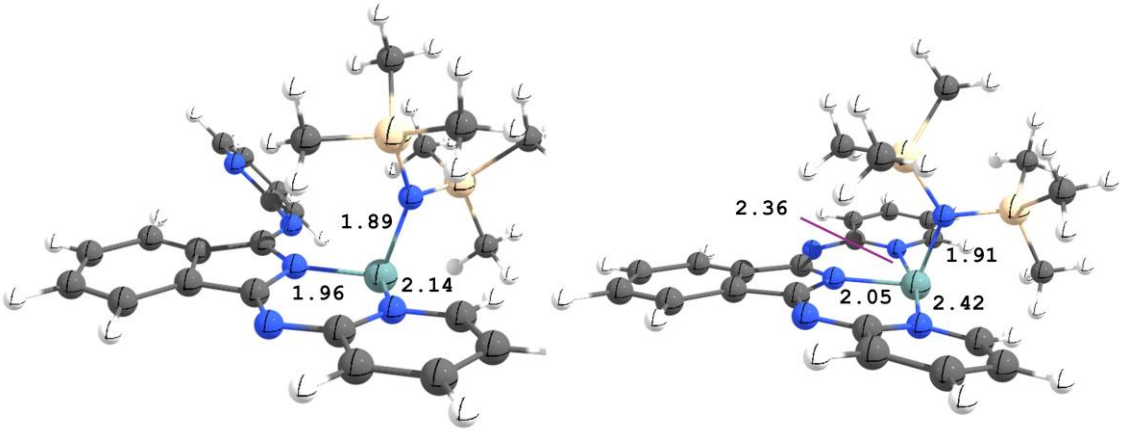

Figure S05. Calculated geometries for two conformers of **1-H** with selected bond lengths in Å.

NBO analysis of 2-H

NBO analysis was conducted with the NBO6.0 program[22] using previously calculated densities at the SMD-B3LYP/6-311+(2d,p) level of theory.

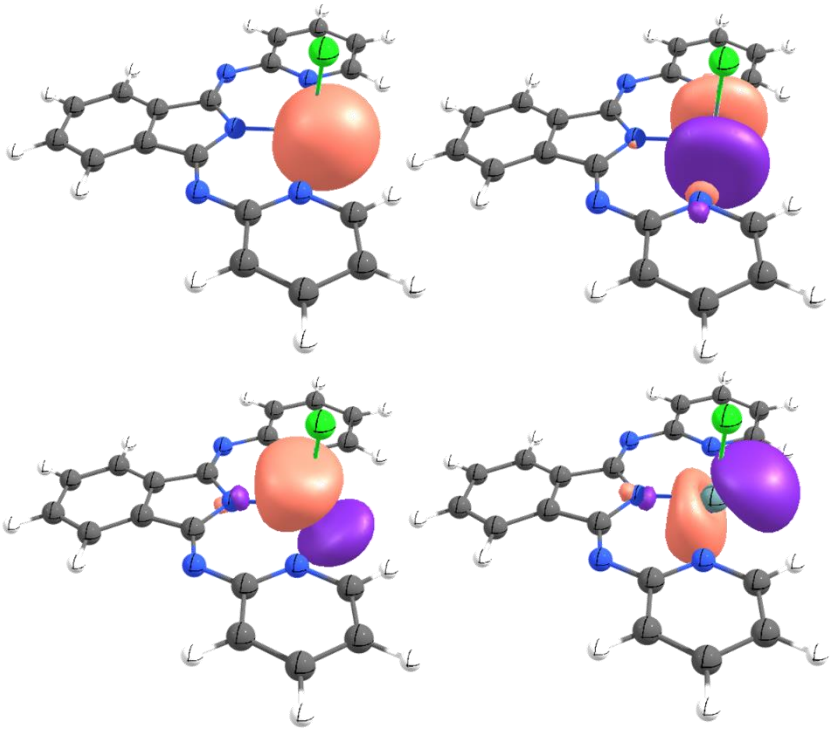

Figure S06. Relevant NBOs of **2-H**, localized on the germanium atom. From top left to bottom right: *s* Lone Pair, *p* Lone Vacancy along the N_{py}–Ge–N_{py} axis, *p* Lone Pairs on the plane perpendicular to the N_{py}–Ge–N_{py} axis.

Charge distribution in 5-H

To model the dimeric species **5-H**, we preserved the $[BPI_2Ge_2]^{2-}$ core, the two potassium cations, and the three THF molecules of the asymmetric unit of the XRD structure. An additional THF molecule was included to reproduce the coordination environment of one of the potassium cations. Free optimization of this model retains the essential structural features of the solid-state structure. We performed MO and NBO analysis on this model, as well as on the planar fragments **BPIGe**$^+$, **BPIGe**, and **BPIGe**$^-$, the latter two resulting from the formal one- and two-electron reductions of the former. **Figure S07** illustrates the NBO charges (in black), the bond distances (in Å, shown in pink charcters), and Wiberg bond indices (in parenthesis) of selected atoms and bonds.

In addition, representations of the LUMO, SOMO, and HOMO of **BPIGe**$^{+}$, **BPIGe**, and **BPIGe**$^{-}$, respectively, are included with their optimized geometries. These highlight that the reduction processes take place at the BPI ligand for these fragments, as discussed for **1-H** and **2-H**. Comparison of the above parameters indicates that the negative charge builds up at the ligand, more notably at the pyridinic and iminic nitrogens. Changes in bond distances and Wiberg bond indices align with the spatial distribution of the LUMO of BPIGe^{+}, which becomes populated upon reduction.

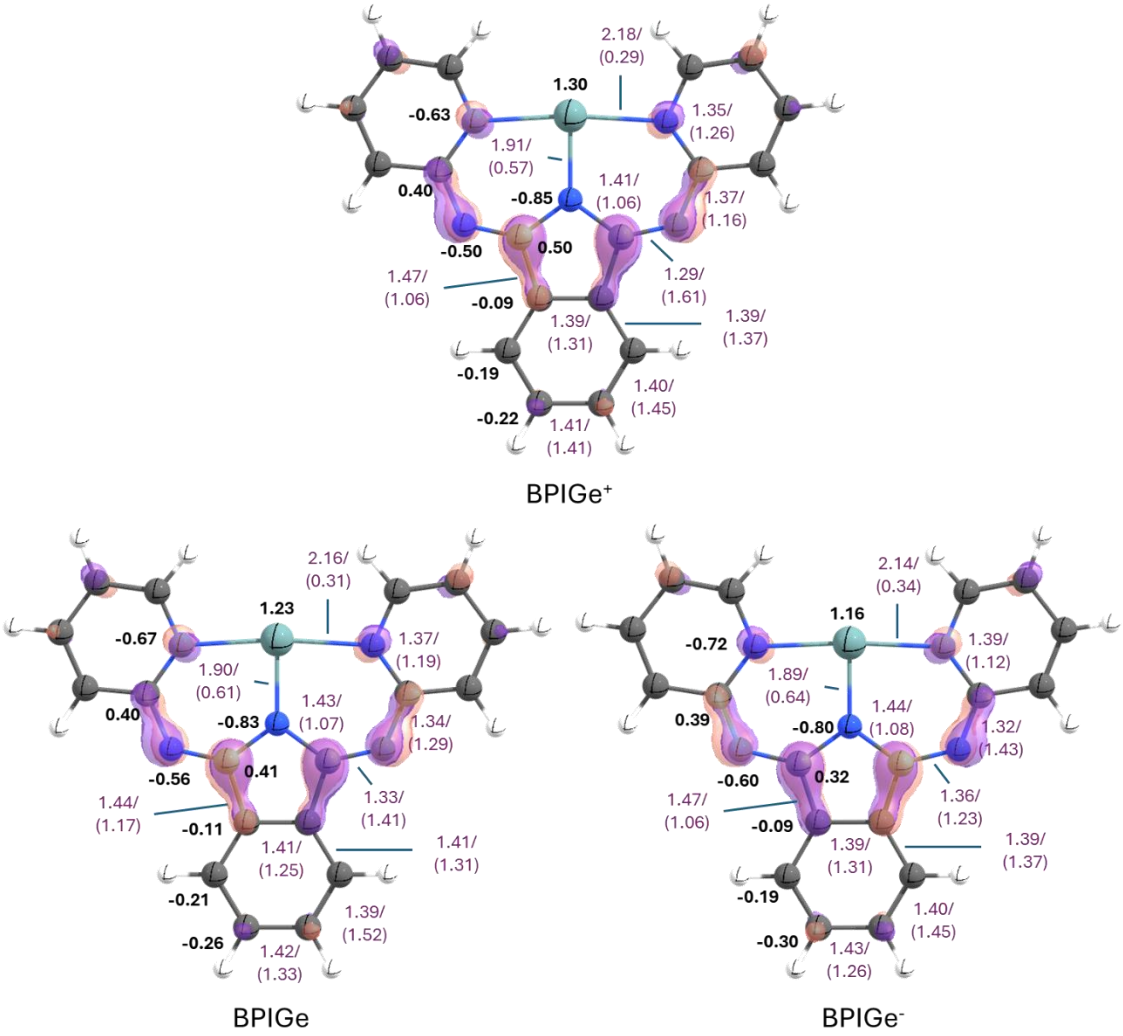

Figure S07. MO and NBO analysis of **BPIGe**$^{+}$, **BPIGe**, and **BPIGe**$^{-}$. These species have C_{2V} symmetry, thus data is shown for one set of the equivalent atoms/bond. NBO charges shown in black, bond distances (in Å) shown in pink, and Wiberg bond indices (in parenthesis) of selected atoms and bonds

Results for our model of **5-H** are shown in **Figure S08**. Consistent with the above results, the HOMO (shown in the figure) and HOMO-1 of the model are localized

one on each BPI ligand, indicating a 4-electron reduction takes place at the BPI ligands of **2**. Now, the BPI ligands are unsymmetric, with each BPI coordinated κ^2 to one germanium atom and κ^1 to the other through one iminic nitrogen. This nitrogen, coordinated to the second germanium atom, bears the highest negative charge, and the bonds to the adjacent carbon atoms are longer than those of the other iminic nitrogen in the same BPI. Close inspection of the HOMO and HOMO-1 of **5-H** reveals that these orbitals are partially localized on the iminic nitrogen atoms bonded to germanium, and along the N_{iminic}—C_{Py} bond (as in $BPIGe^-$). Further, NBO analysis locates two lone pairs on the first type of iminic nitrogen and one on the second type, suggesting that one of the two iminic nitrogen atoms on each BPI has amide character. Additionally, NBO analysis locates one *s-lone pair* and three *p-lone vacancies* on each germanium atom, supporting the notion of **5-H** being a Ge(II) species (**Figure S09**).

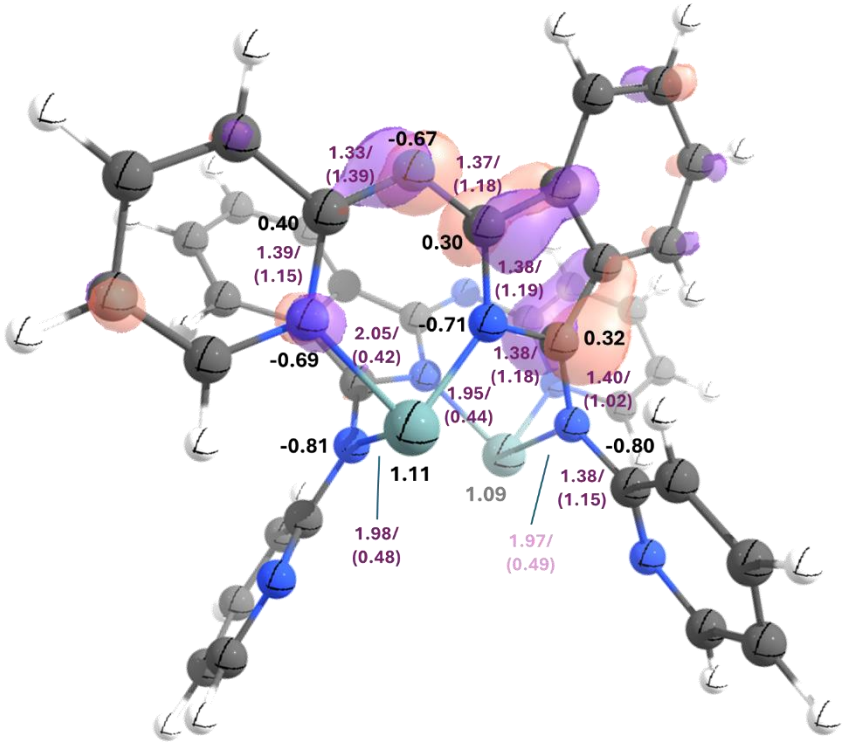

Figure S08. MO and NBO analysis of model **5-H**. K^+ ions and THF molecules are omitted for clarity. NBO charges (in black), bond distances in Å (shown in pink), and Wiberg bond indices (in parenthesis) of selected atoms and bonds

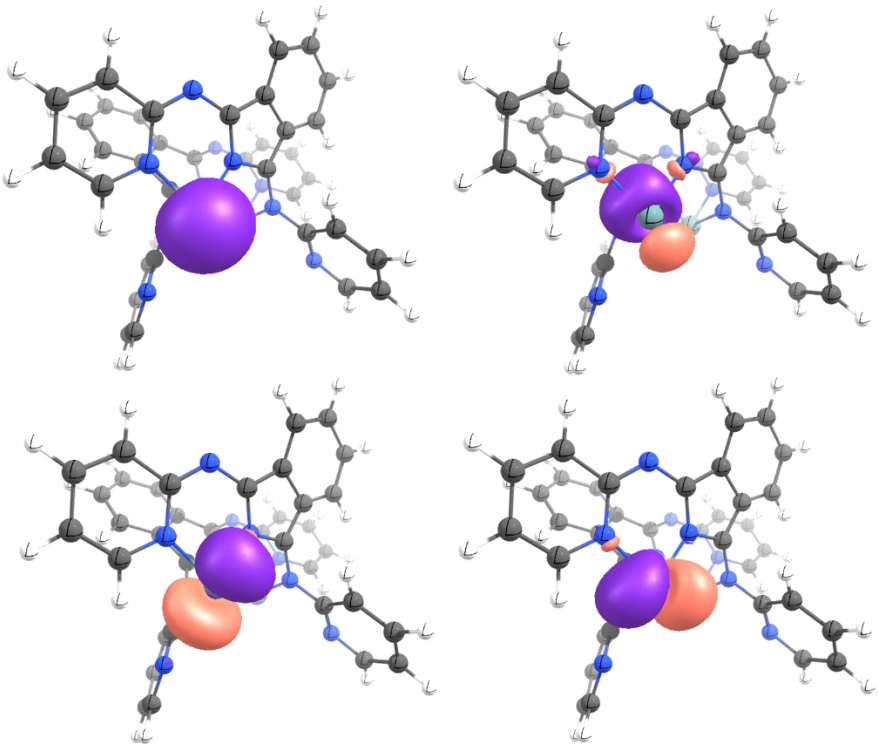

Figure S09. Lone pair (top left) and lone vacancies on one of the germanium atoms of model **5-H**. K^+ ions and THF molecules are omitted for clarity.

NMR spectra of new compounds

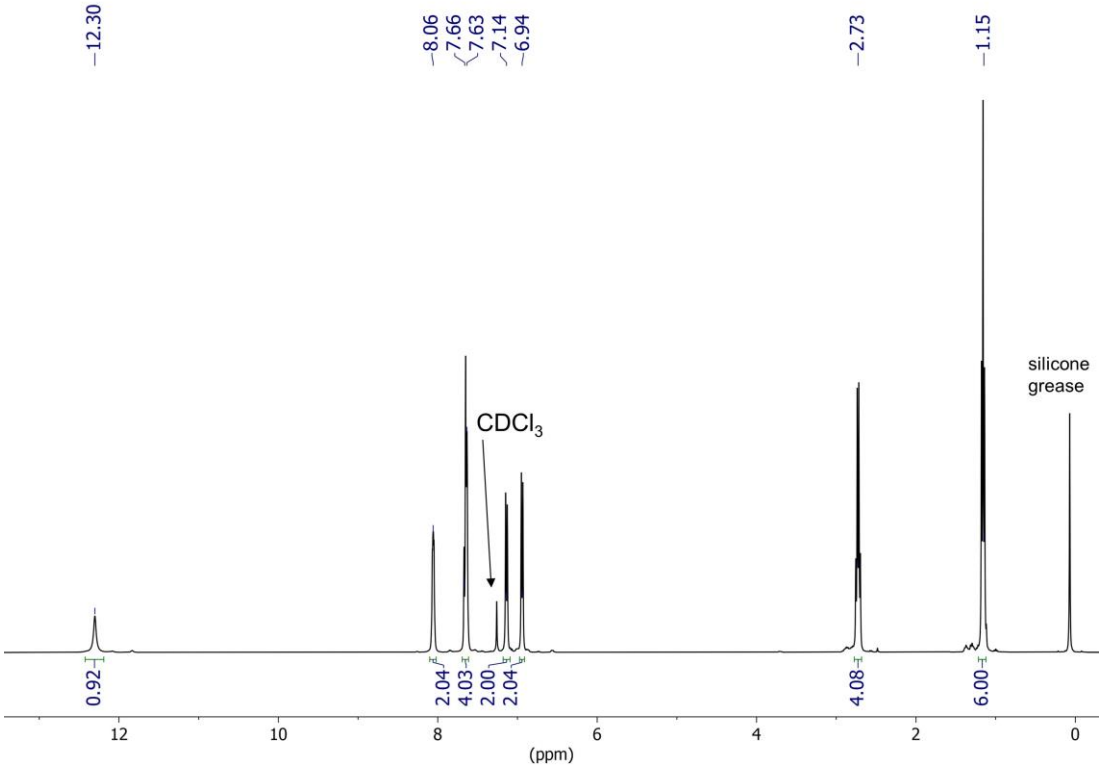

Figure S10. ^{1}H NMR (400 MHz, $CDCl_3$, 25 °C) of ligand **^{Et}HBPI**.

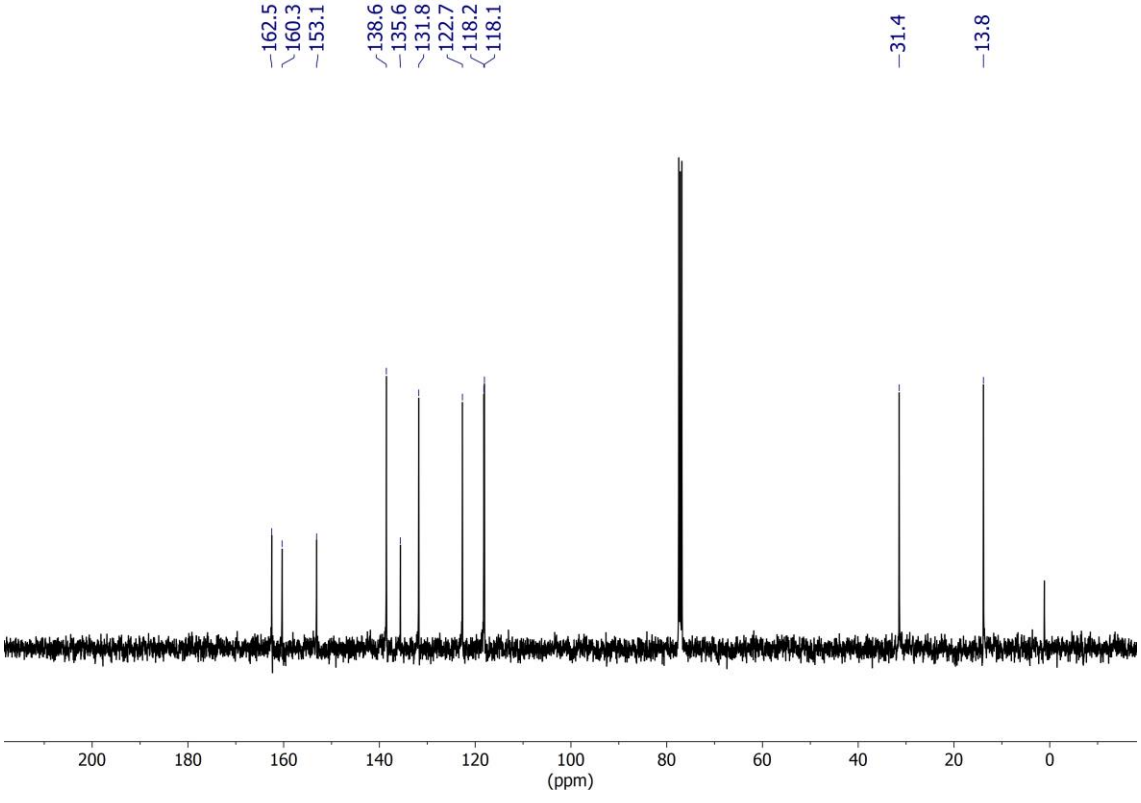

Figure S11. $^{13}C\{^{1}H\}$ NMR (100 MHz, $CDCl_3$, 25 °C) of ligand **^{Et}HBPI**.

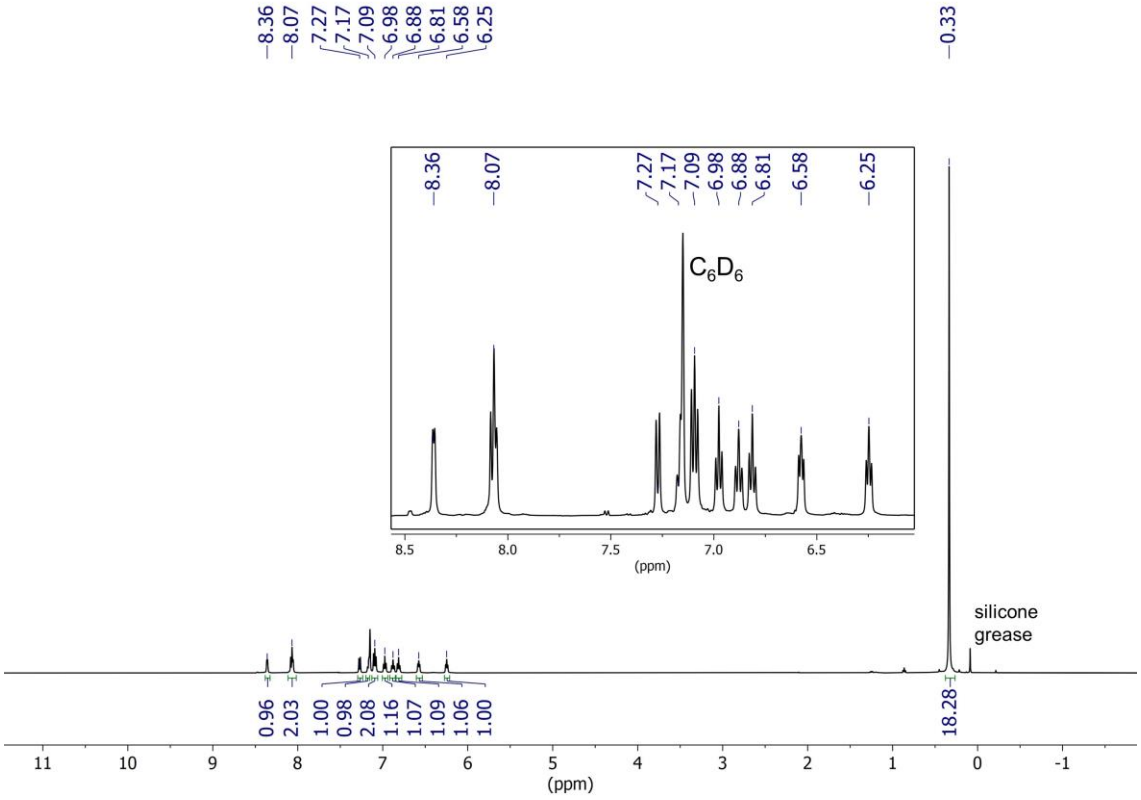

Figure S12. ^{1}H NMR (500 MHz, C_6D_6, 25 °C) of complex **1-H**.

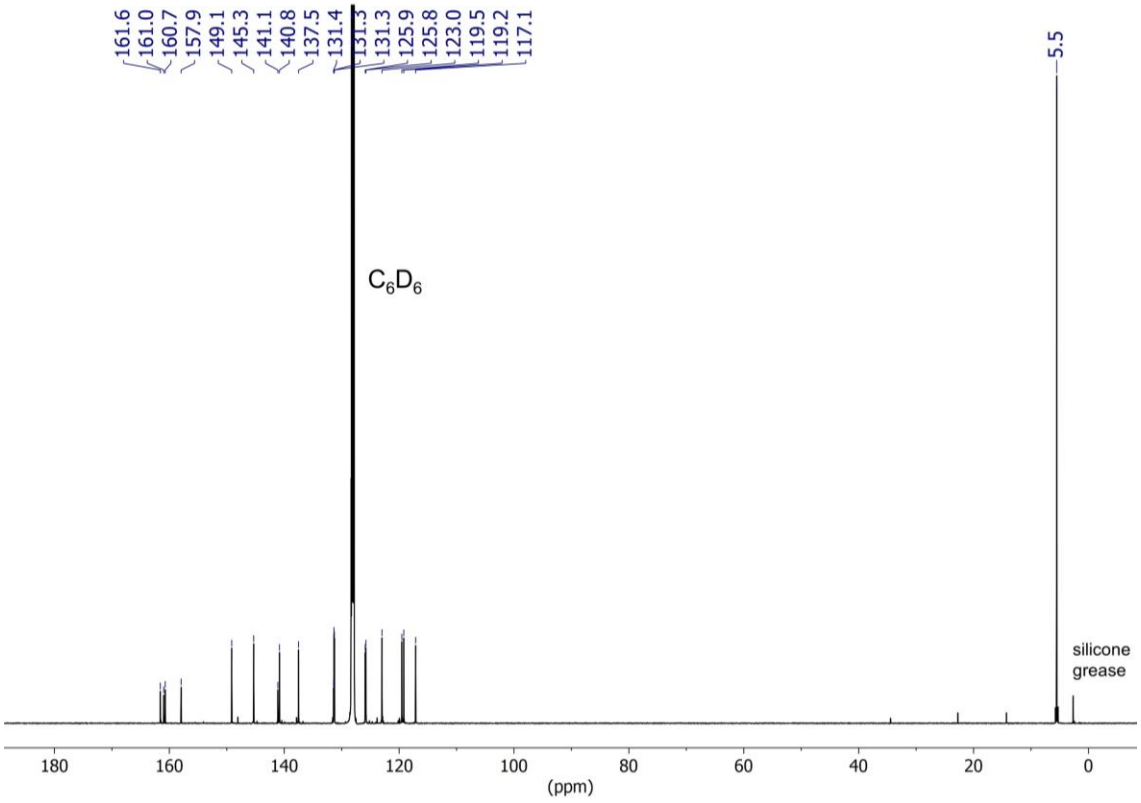

Figure S13. $^{13}C\{^{1}H\}$ NMR (125 MHz, C_6D_6, 25 °C) of complex **1-H**.

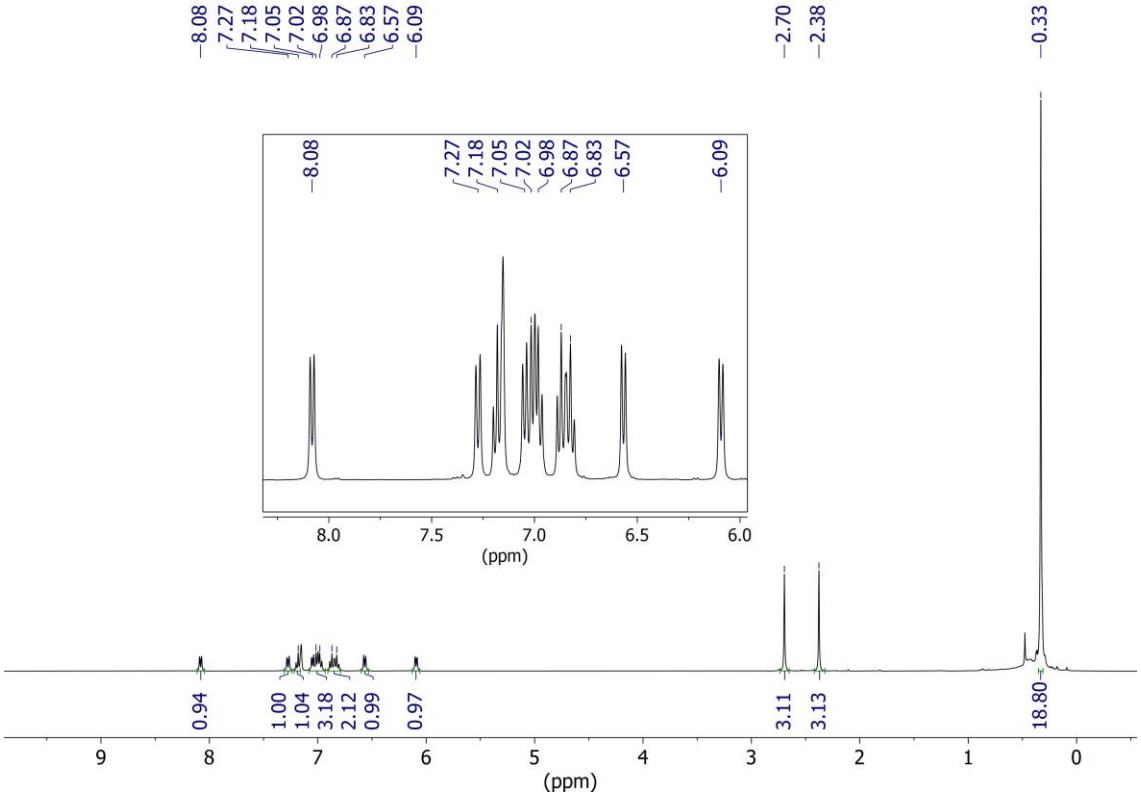

Figure S14. ^{1}H NMR (400 MHz, C_6D_6, 25 °C) of complex **1-Me**.

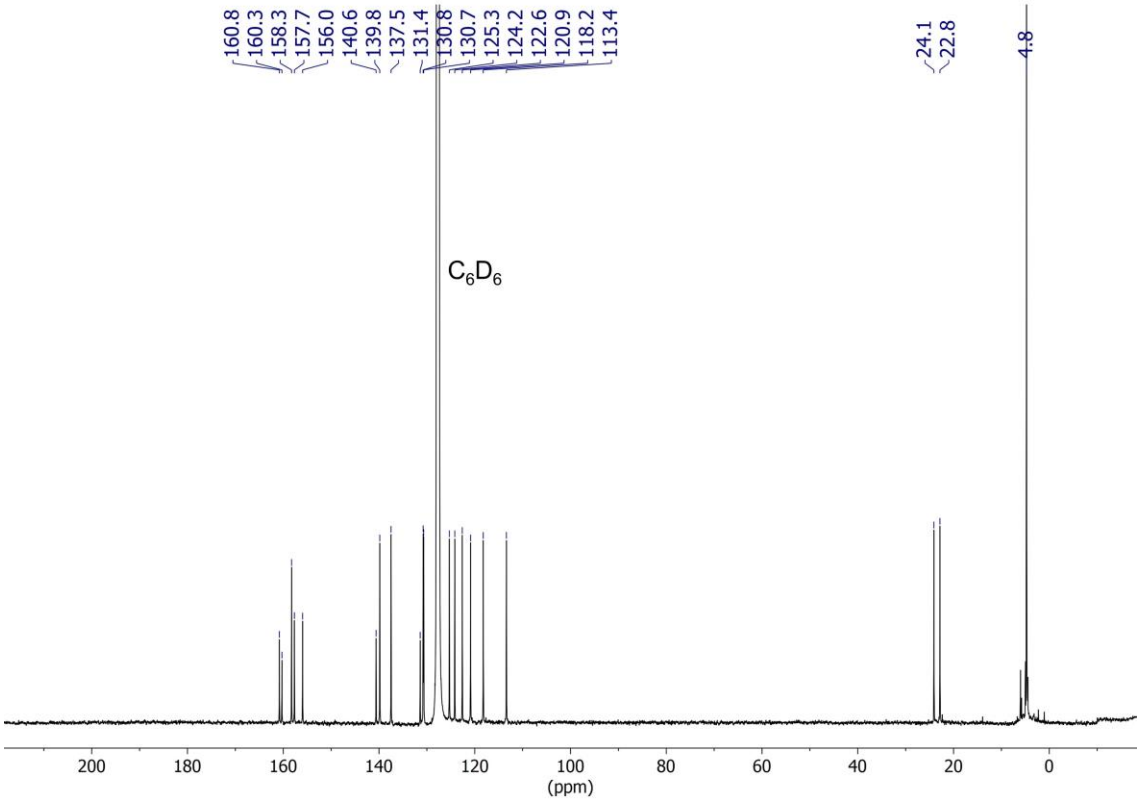

Figure S15. ^{13}C{^{1}H} NMR (100 MHz, C_6D_6, 25 °C) of complex **1-Me**.

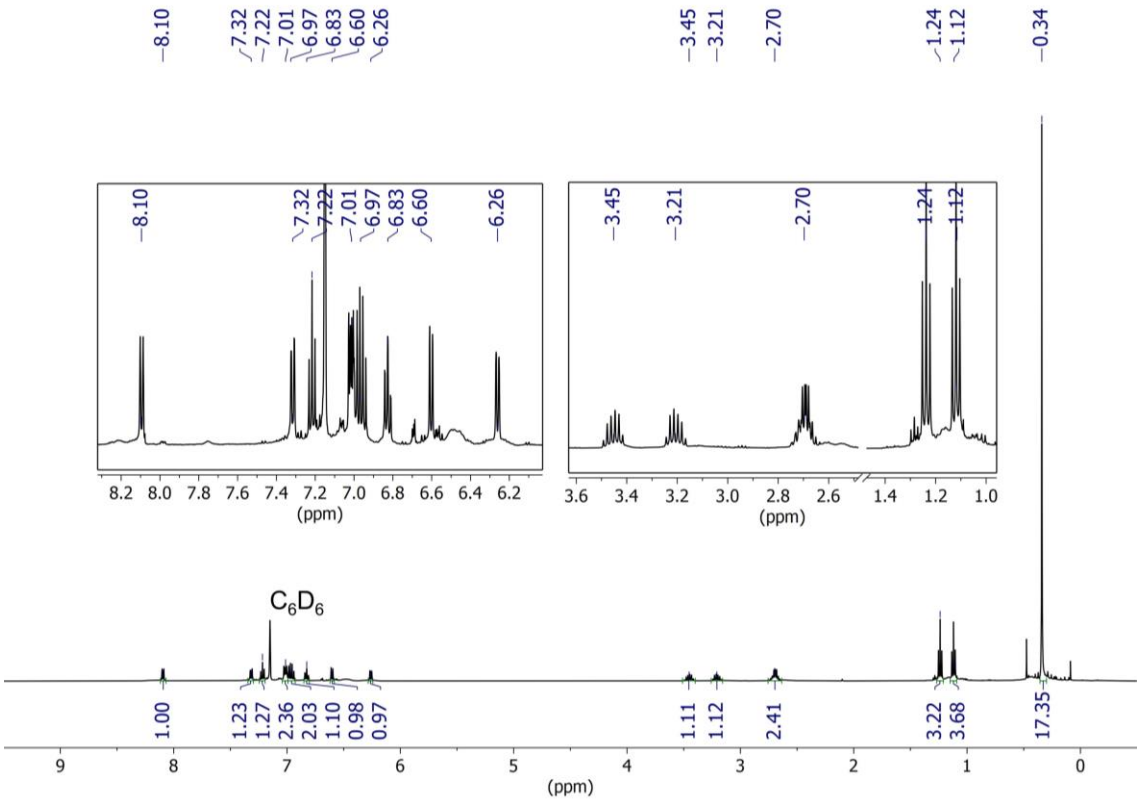

Figure S16. ^{1}H NMR (500 MHz, C_6D_6, 25 °C) of complex **1-Et**.

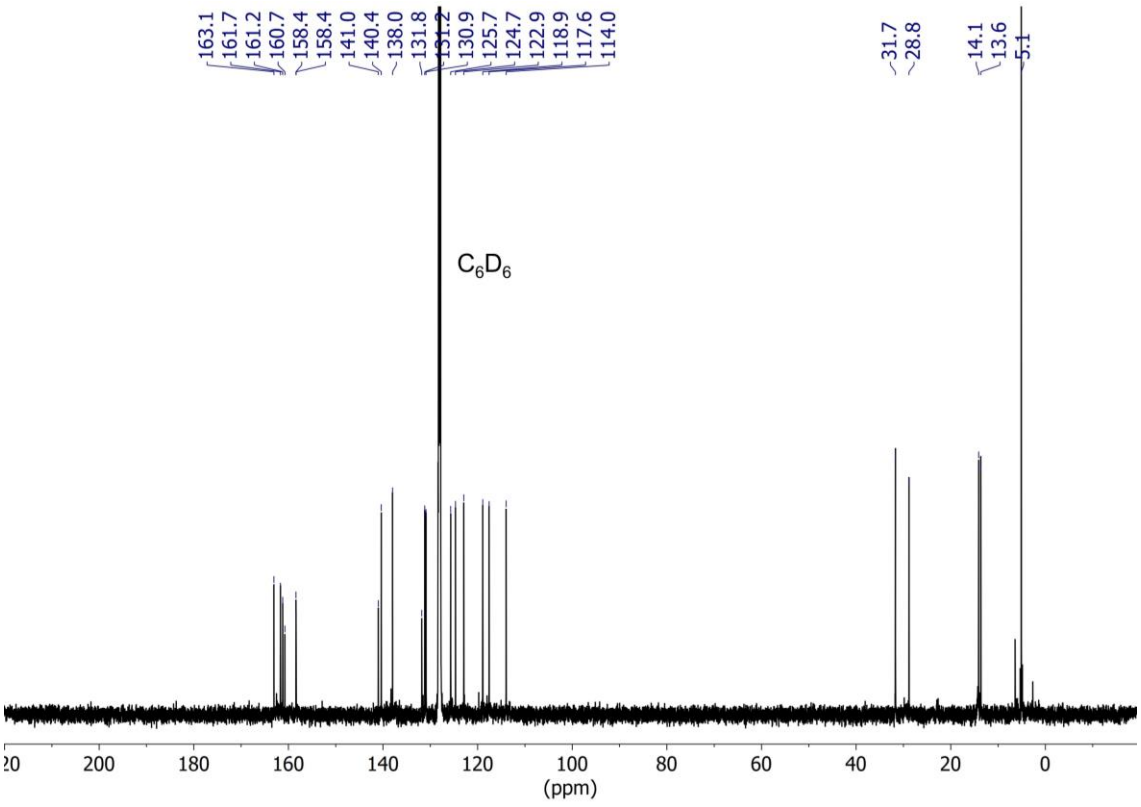

Figure S17. $^{13}C\{^{1}H\}$ NMR (125 MHz, C_6D_6, 25 °C) of complex **1-Et**.

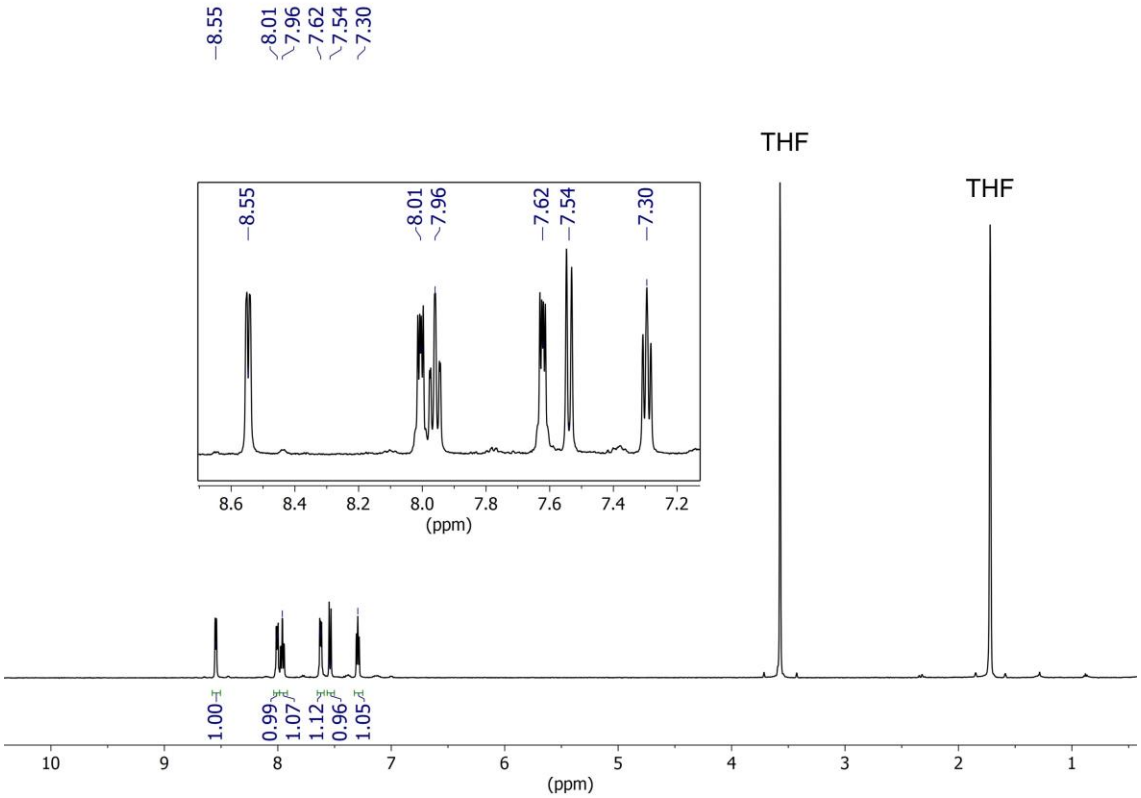

Figure S18 ^{1}H NMR (500 MHz, THF-d_8, 25 °C) of complex **2-H**.

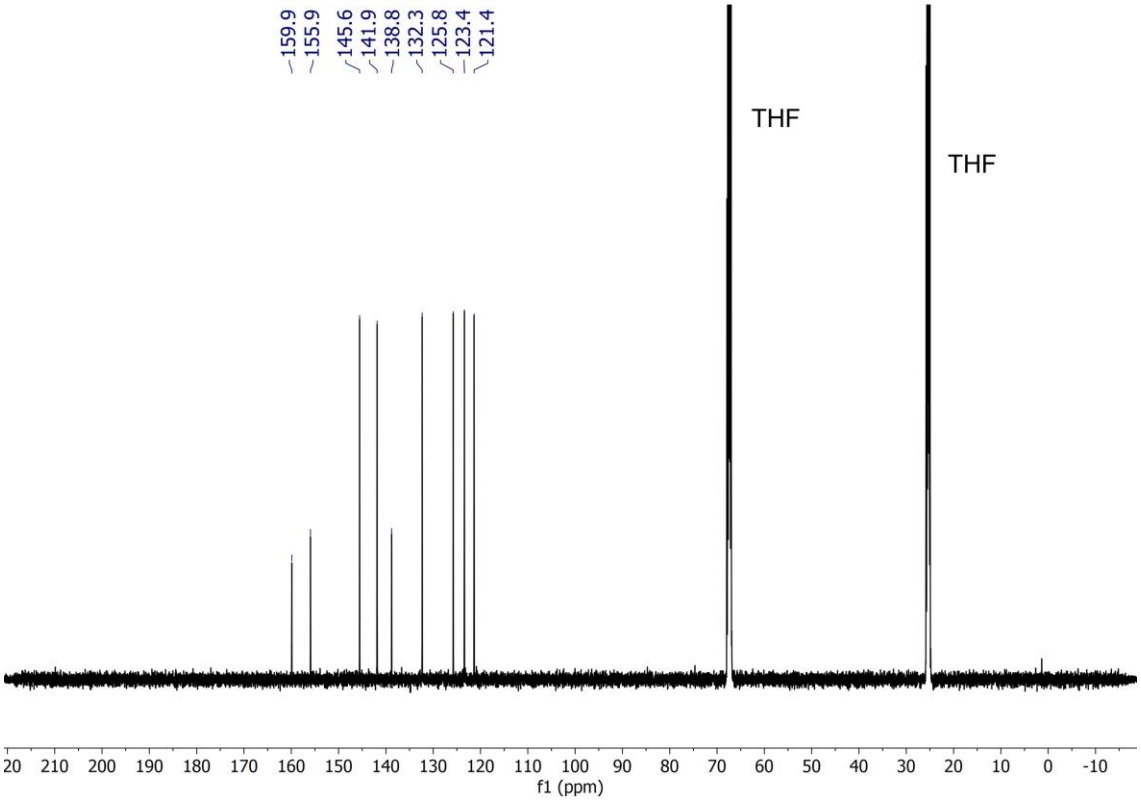

Figure S19. ^{13}C{^{1}H} NMR (125 MHz, THF-d_8, 25 °C) of complex **2-H**.

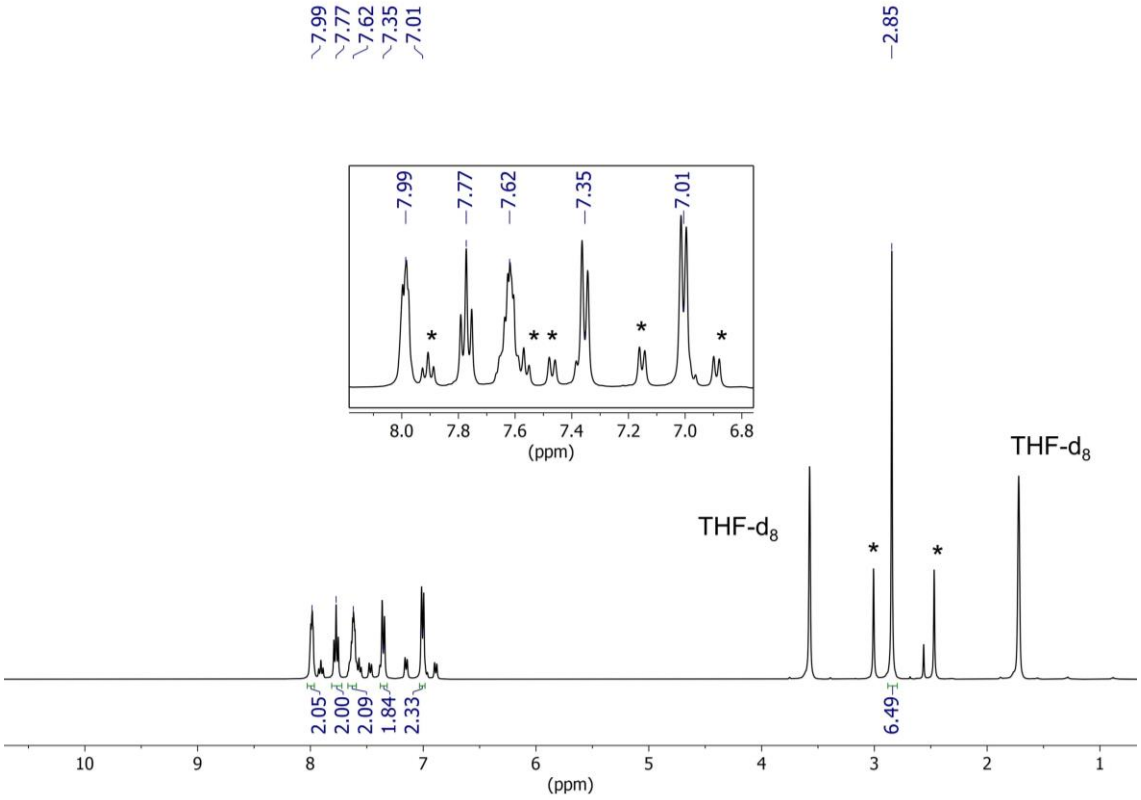

Figure S20 ^{1}H NMR (400 MHz, THF-d_8, 25 °C) of complex **2-Me**. * represents the minor isomer discussed in the main text.

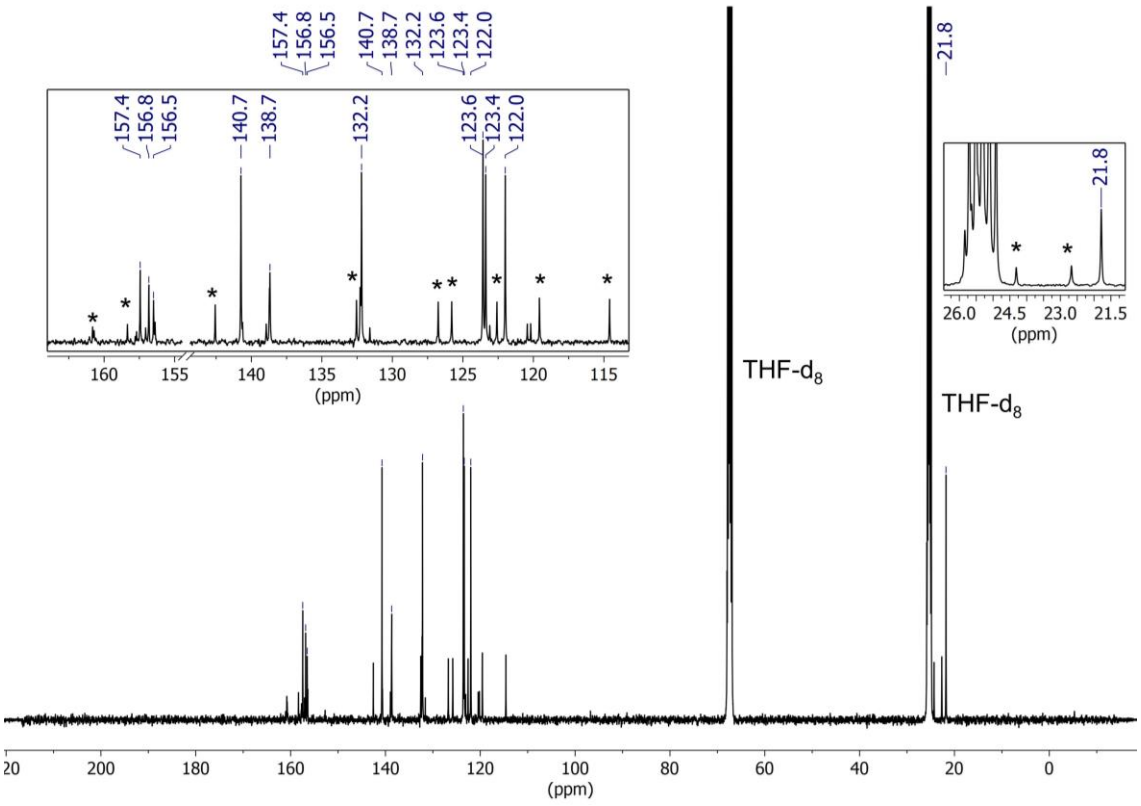

Figure S21. ^{13}C{^{1}H} NMR (100 MHz, THF-d_8, 25 °C) of complex **2-Me**. * represents the minor isomer discussed in the main text.

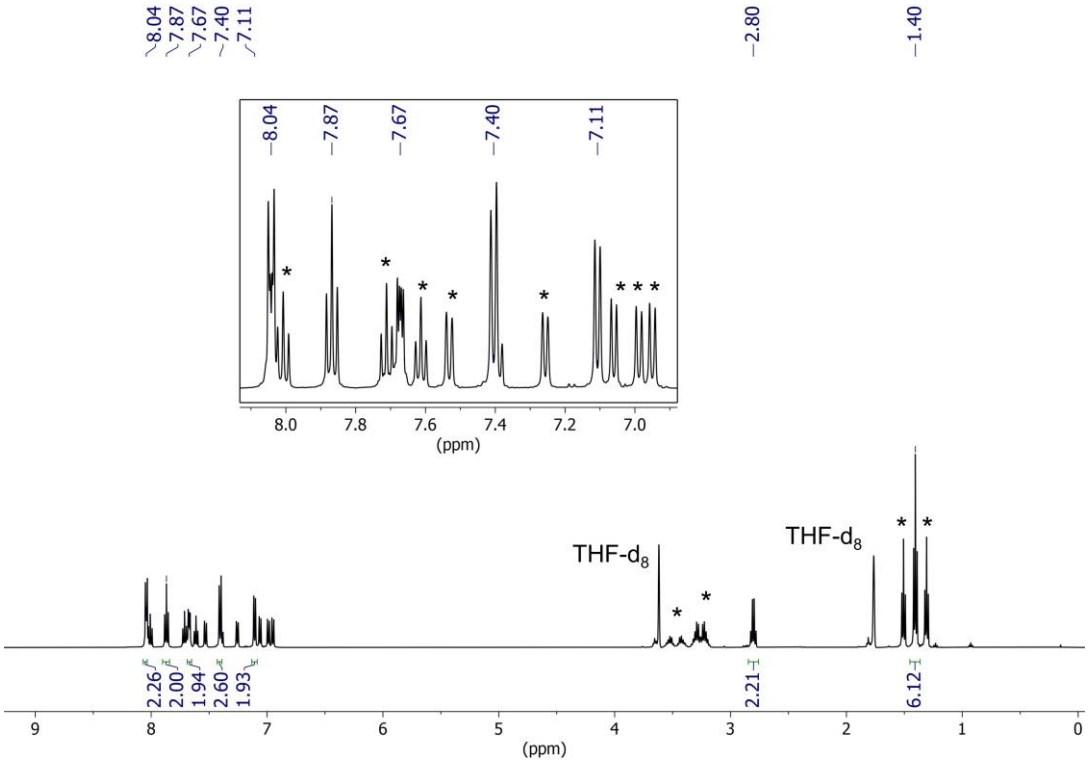

Figure S22 ^{1}H NMR (500 MHz, THF-d_8, 25 °C) of complex **2-Et**. * represents the minor isomer discussed in the main text.

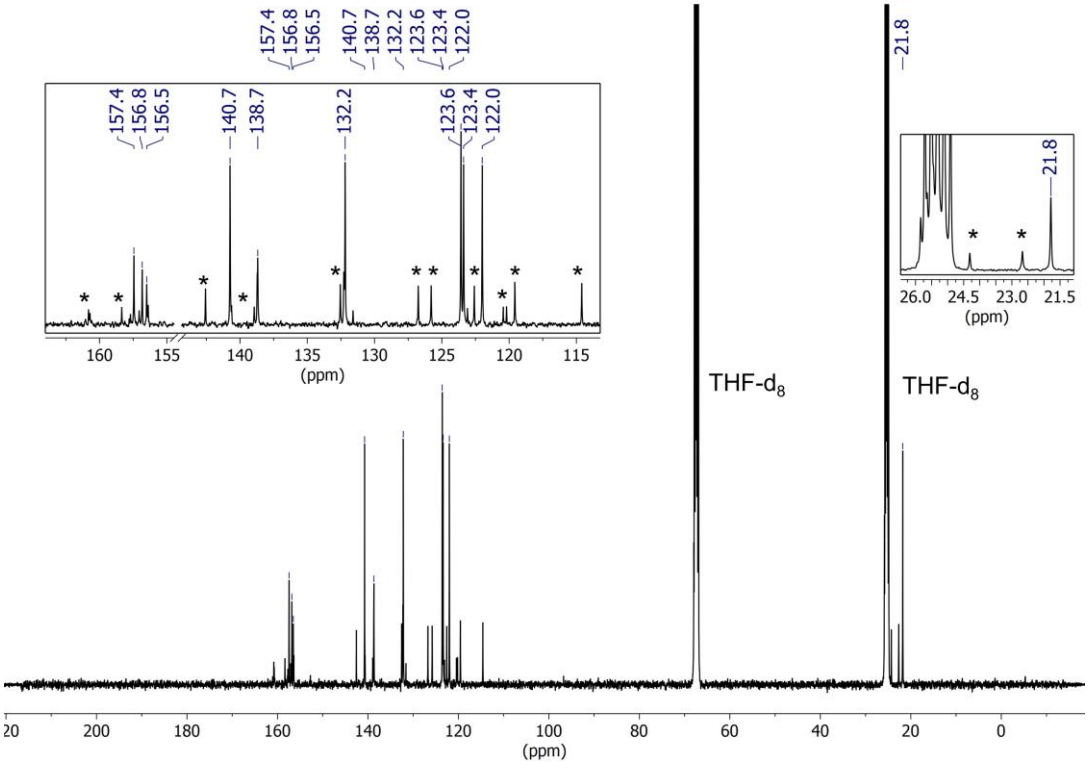

Figure S23. ^{13}C{^{1}H} NMR (125 MHz, THF-d_8, 25 °C) of complex **2-Et**. * represents the minor isomer discussed in the main text.

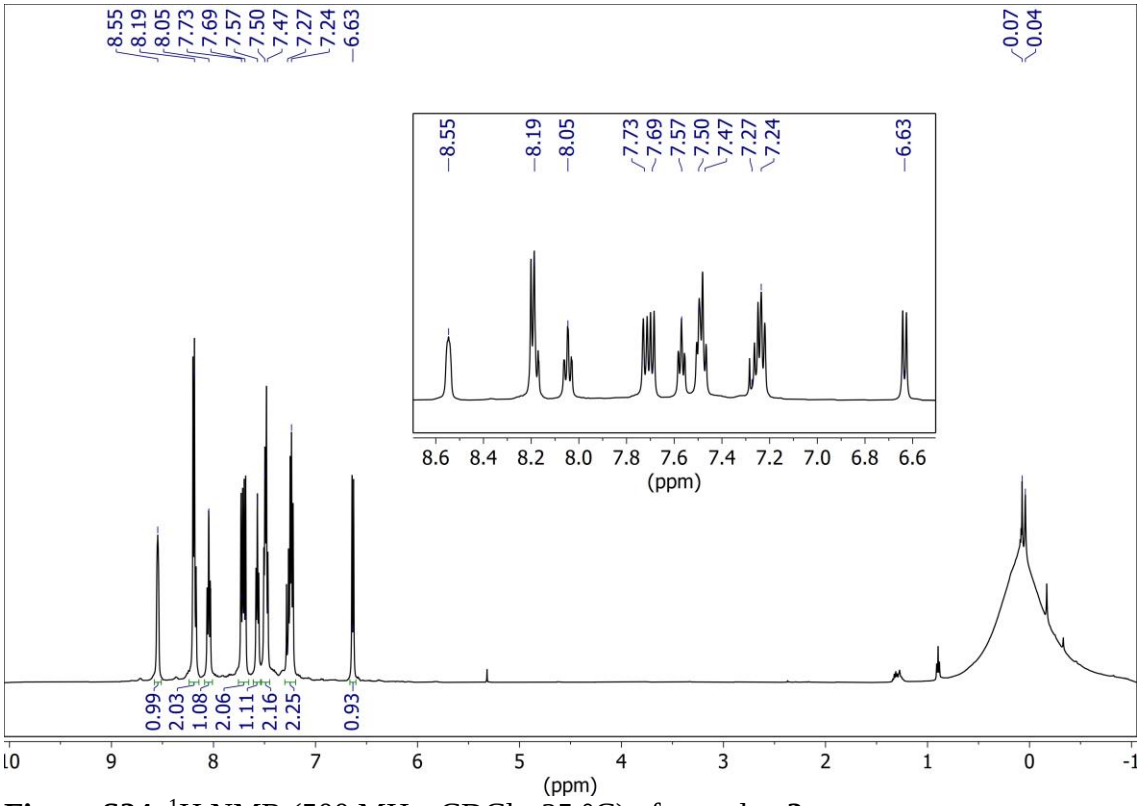

Figure S24. ^{1}H NMR (500 MHz, $CDCl_3$, 25 °C) of complex **3**.

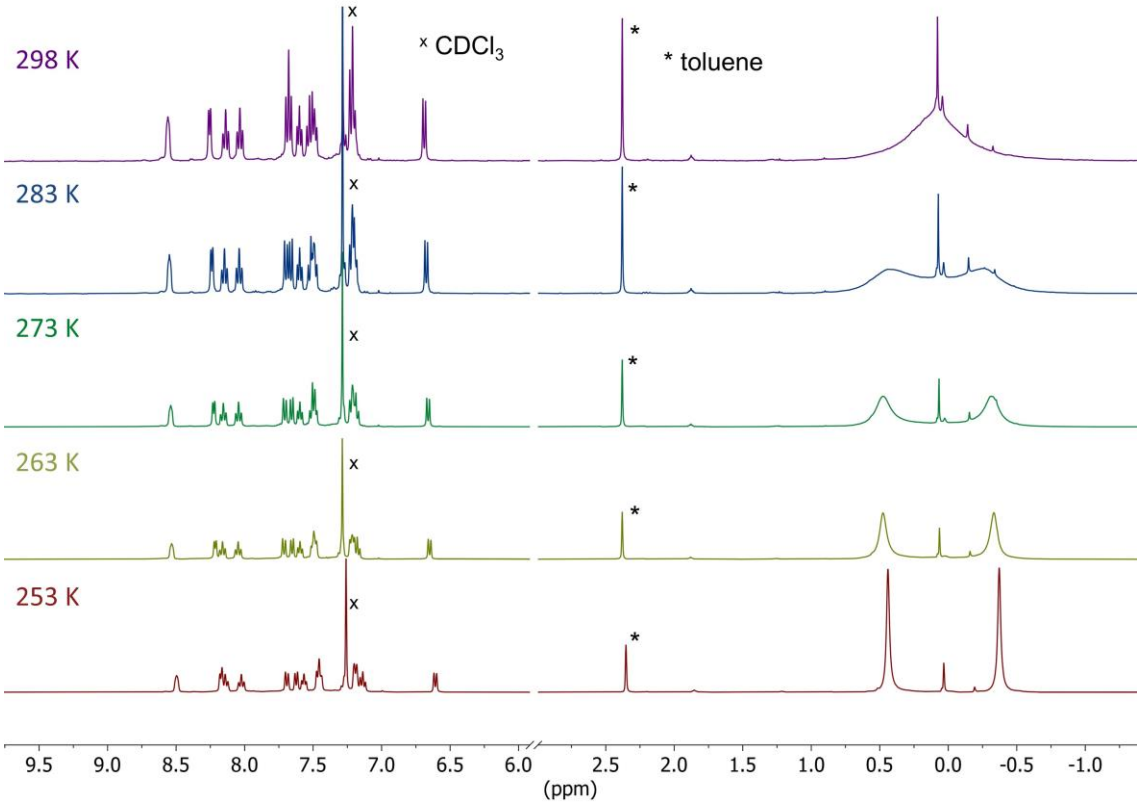

Figure S25. ^{1}H NMR (400 MHz, $CDCl_3$) of complex **3** as a function of the temperature.

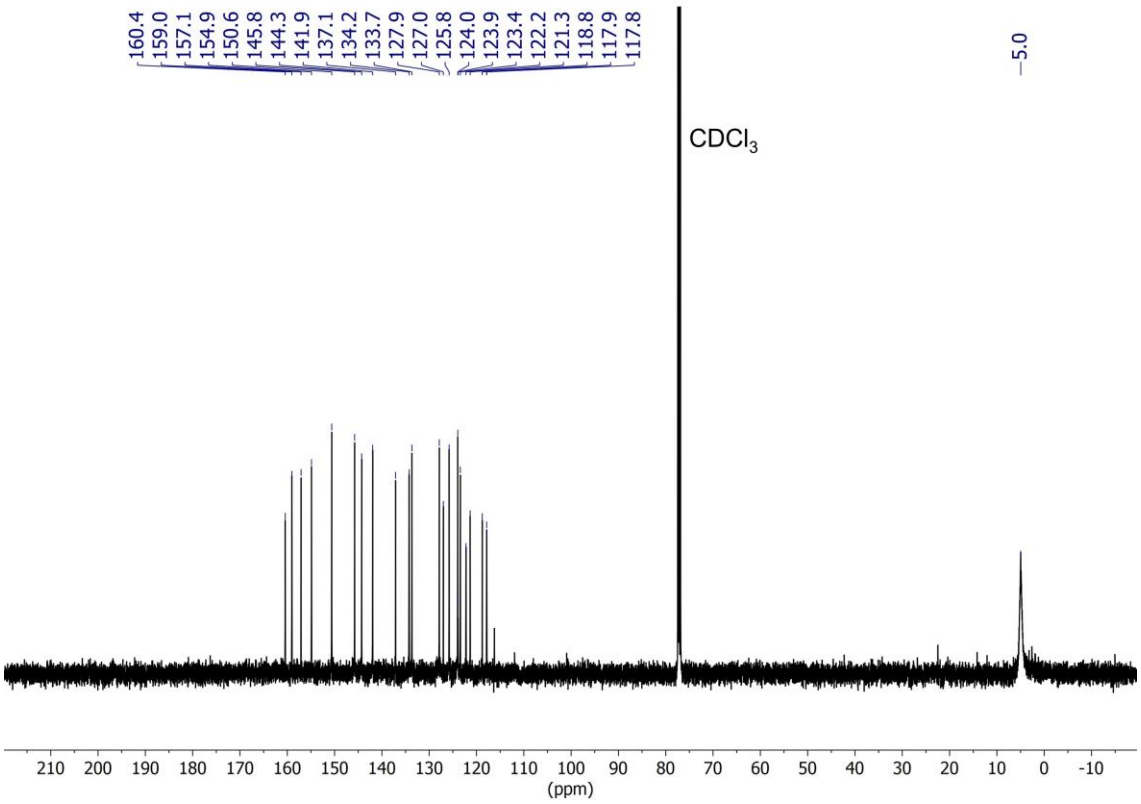

Figure S26. $^{13}C\{^{1}H\}$ NMR (100 MHz, THF-d_8, 25 °C) of complex **3**.

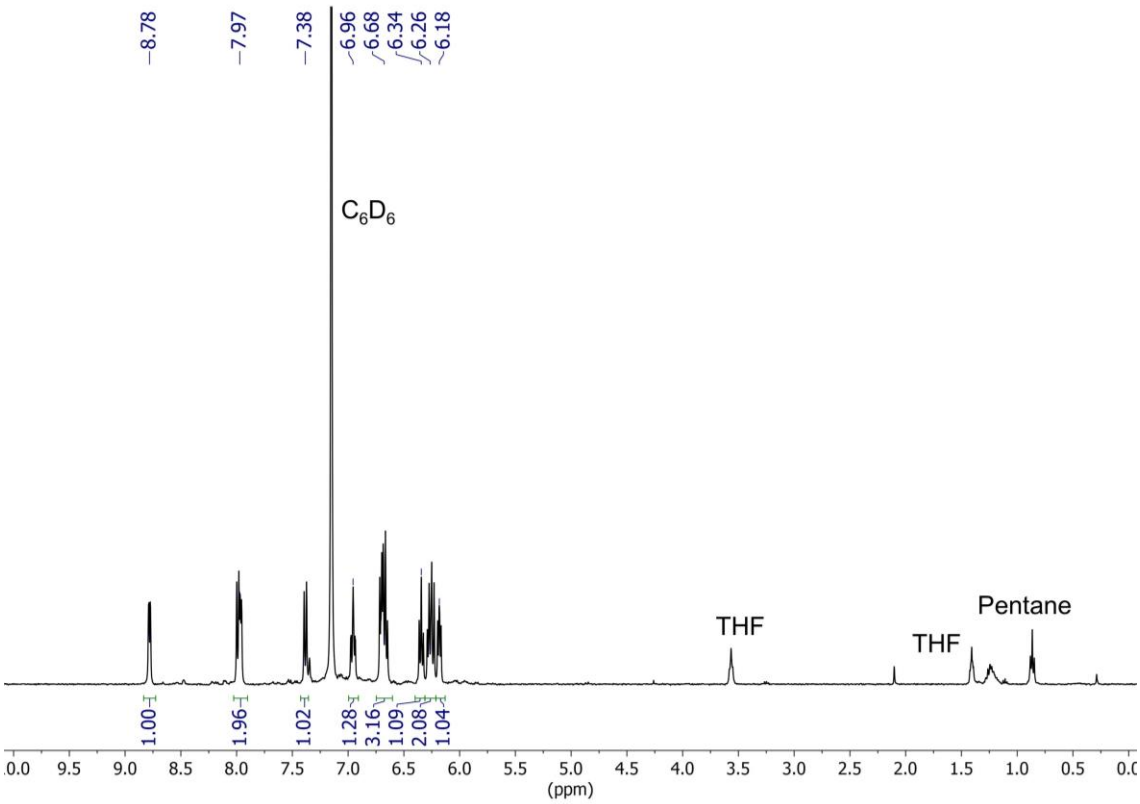

Figure S27 ^{1}H NMR (400 MHz, C_6D_6, 25 °C) of complex **4-H**.

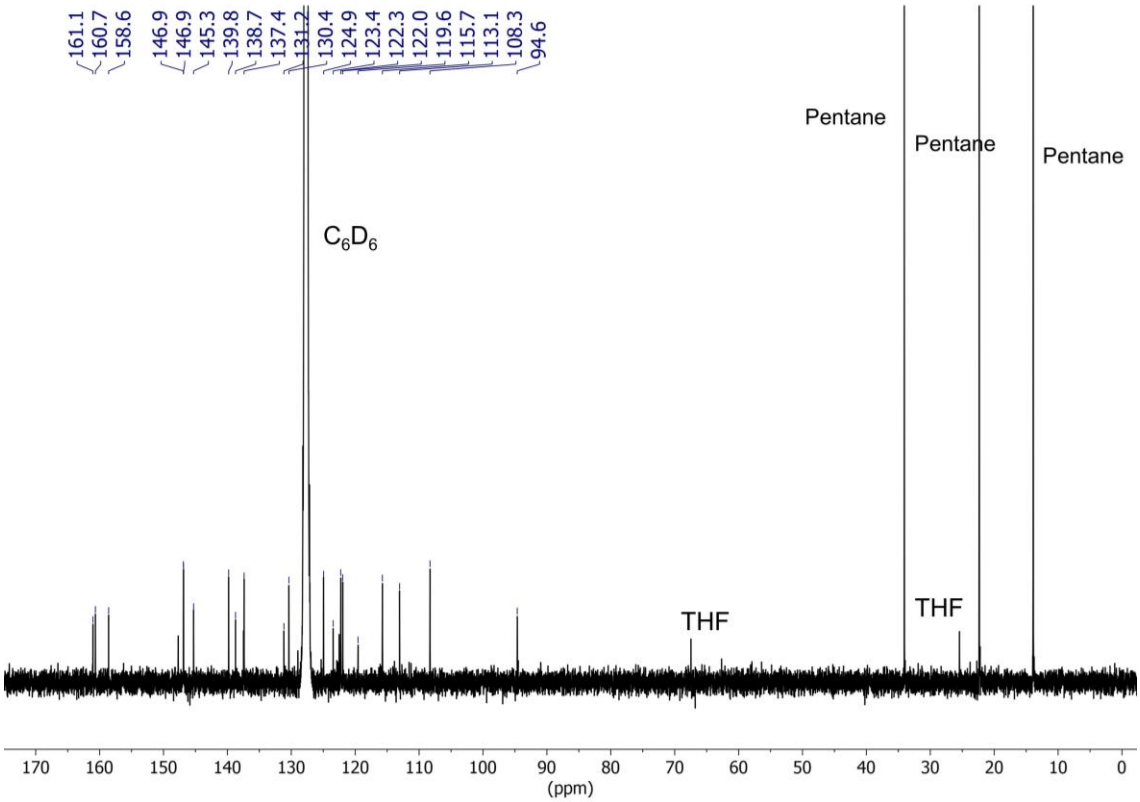

Figure S28. $^{13}C\{^{1}H\}$ NMR (500 MHz, C_6D_6, 25 °C) of complex **4-H**.

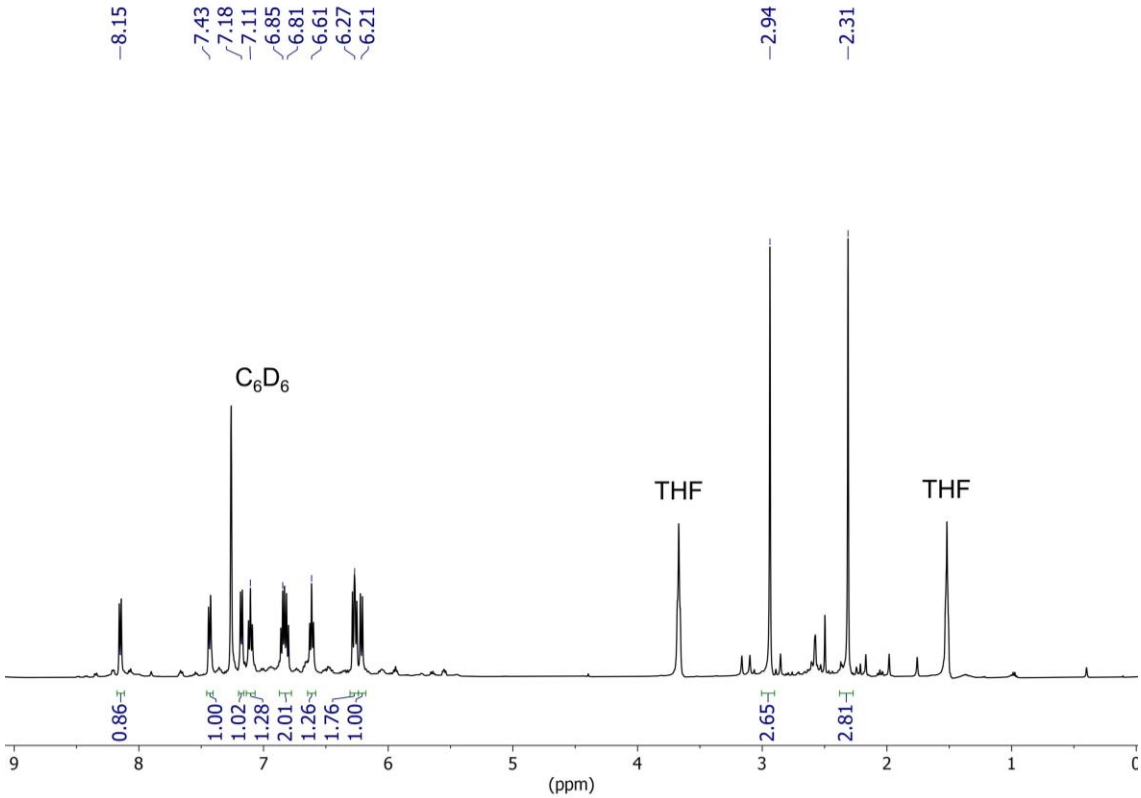

Figure S29. ^{1}H NMR (500 MHz, $CDCl_3$, 25 °C) of complex **4-Me**.

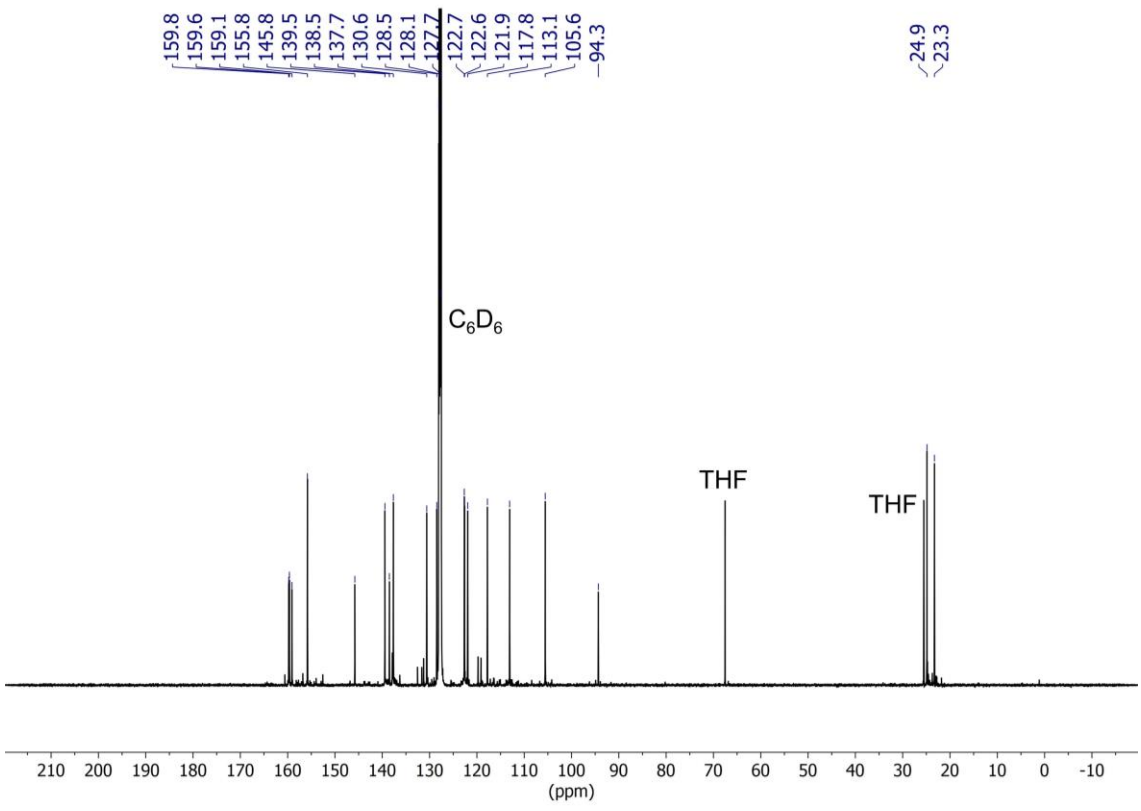

Figure S30. $^{13}C\{^{1}H\}$ NMR (500 MHz, $CDCl_3$, 25 °C) of complex **4-Me**.

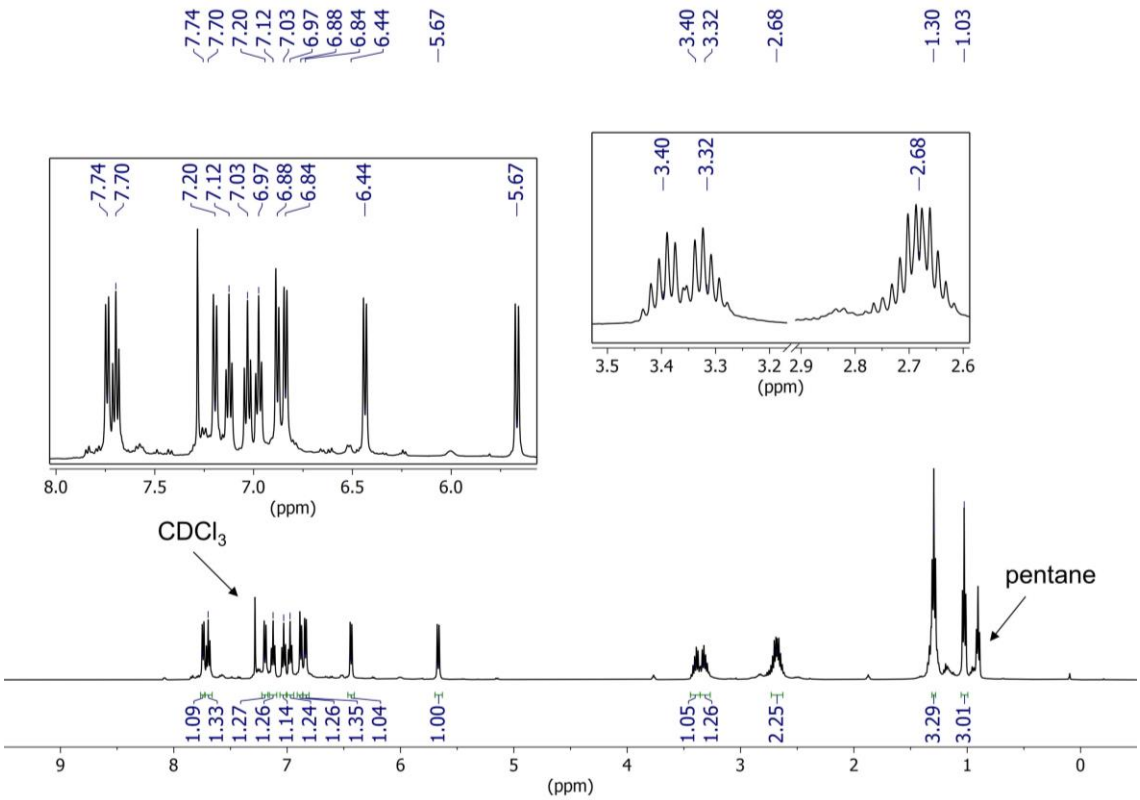

Figure S31. ^{1}H NMR (500 MHz, $CDCl_3$, 25 °C) of complex **4-Et**.

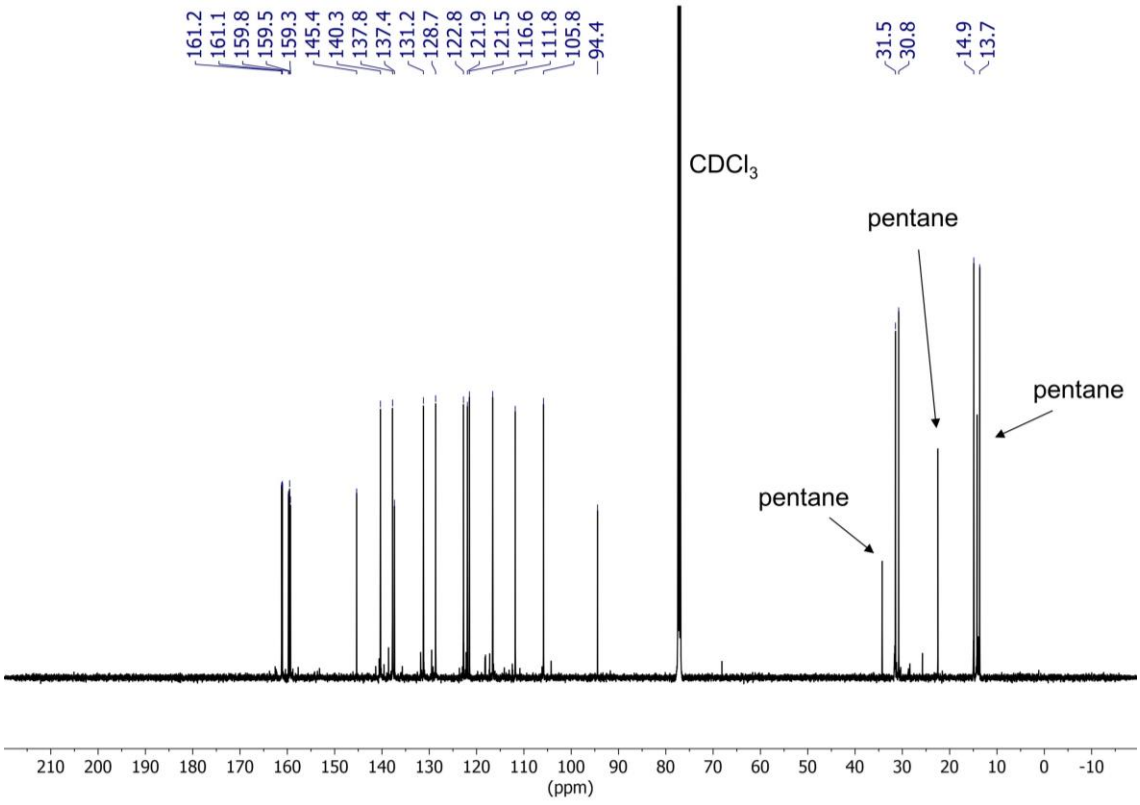

Figure S32. $^{13}C\{^{1}H\}$ NMR (500 MHz, $CDCl_3$, 25 °C) of complex **4-Et**.

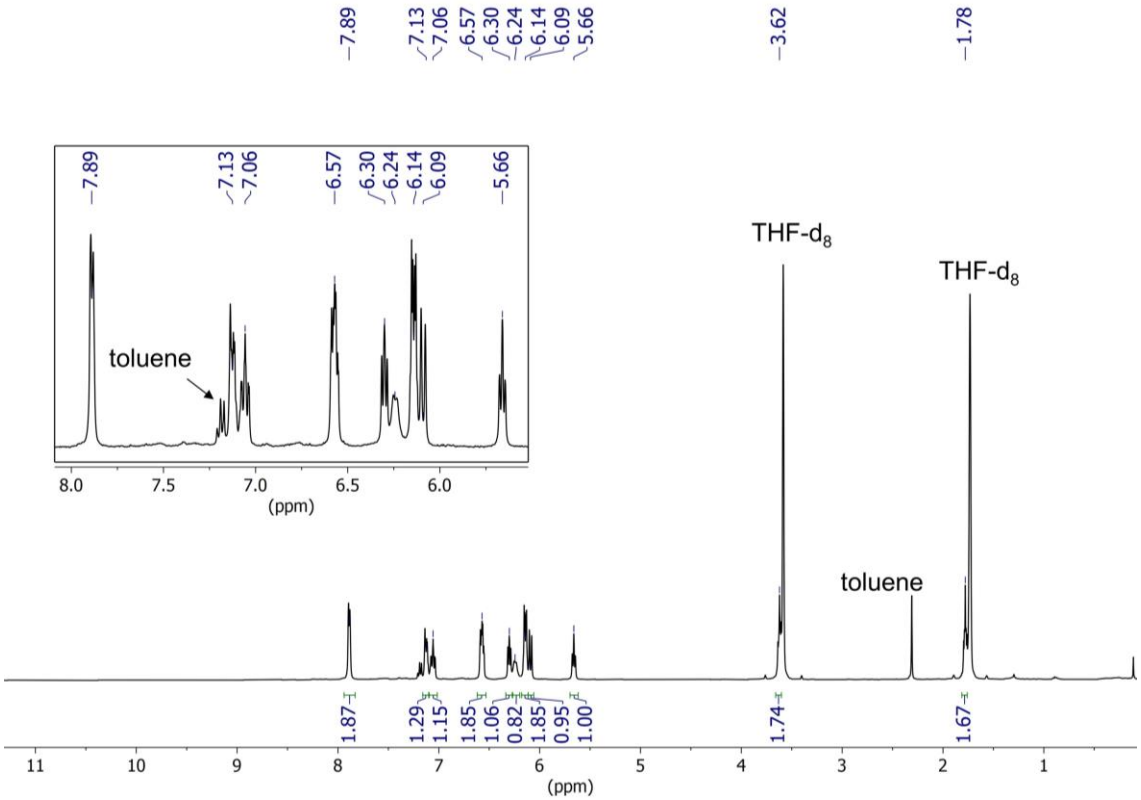

Figure S33. ^{1}H NMR (400 MHz, THF-d_8, 25 °C) of complex **5-H**.

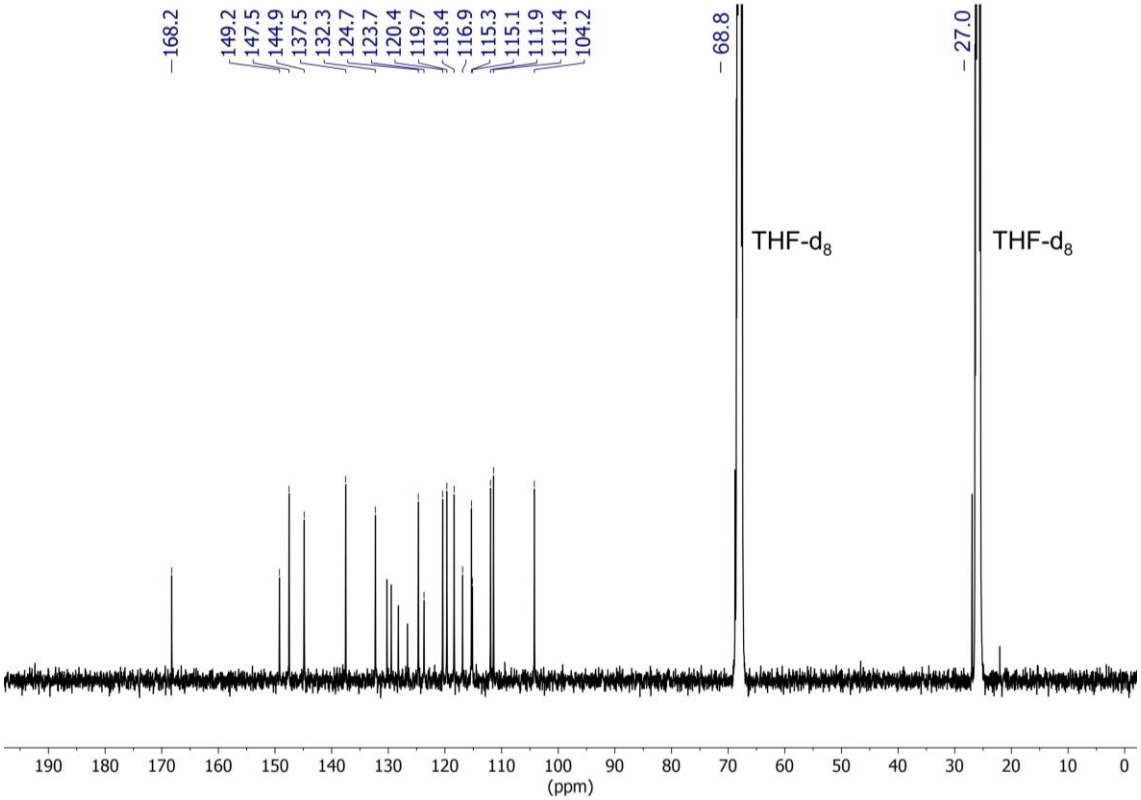

Figure S34. ^{13}C{^{1}H} NMR (100 MHz, THF-d_8, 25 °C) of complex **5-H**.

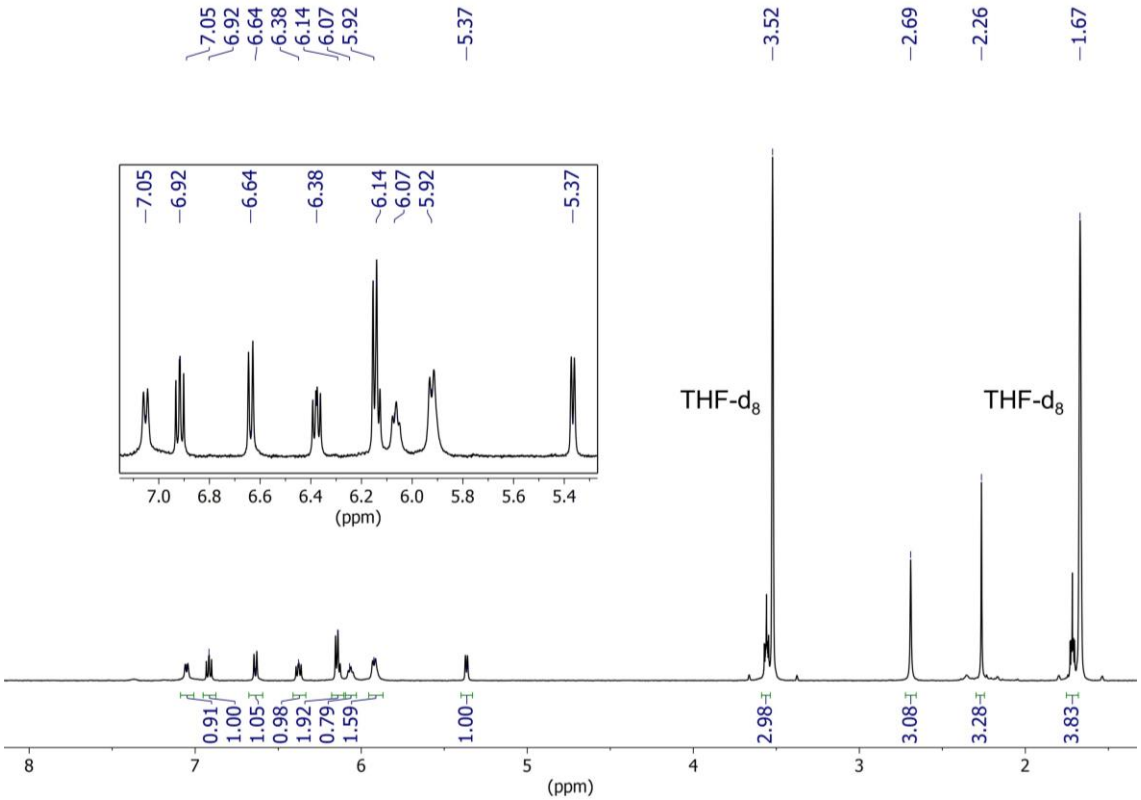

Figure S35. ^{1}H NMR (500 MHz, THF-d_8, 25 °C) of complex **5-Me**.

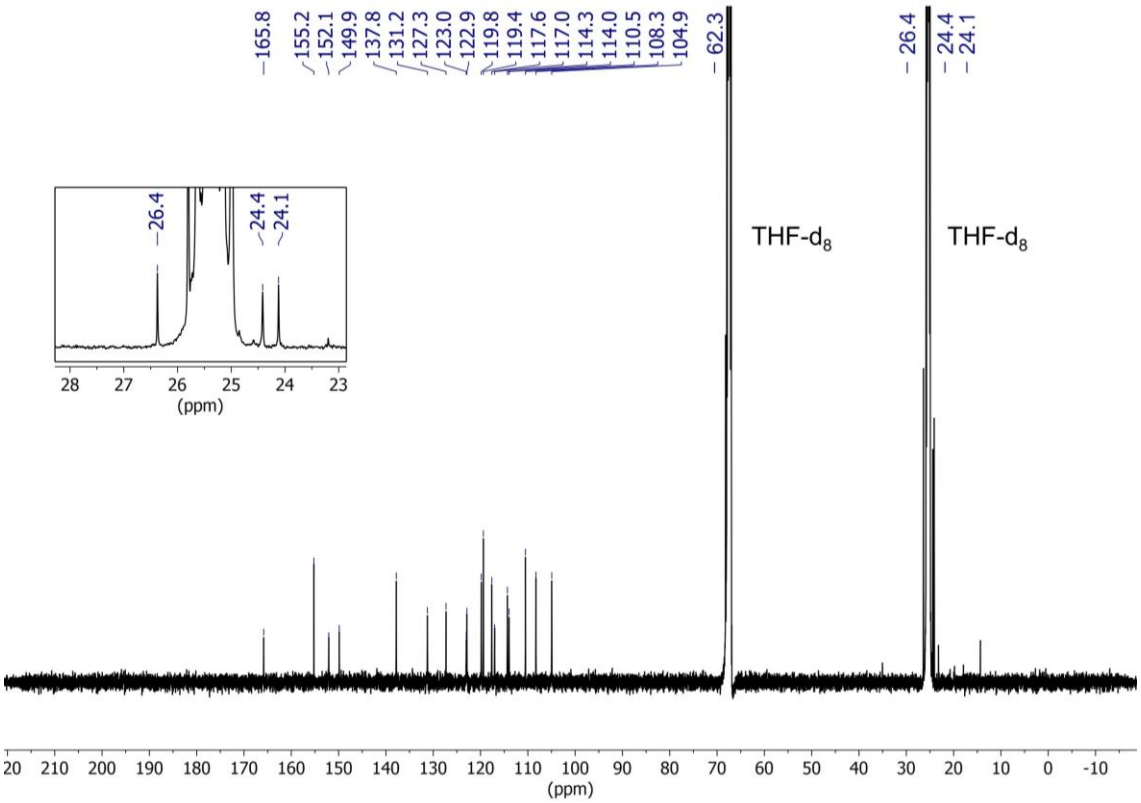

Figure S36. ^{13}C{^{1}H} NMR (125 MHz, THF-d_8, 25 °C) of complex **5-Me**.

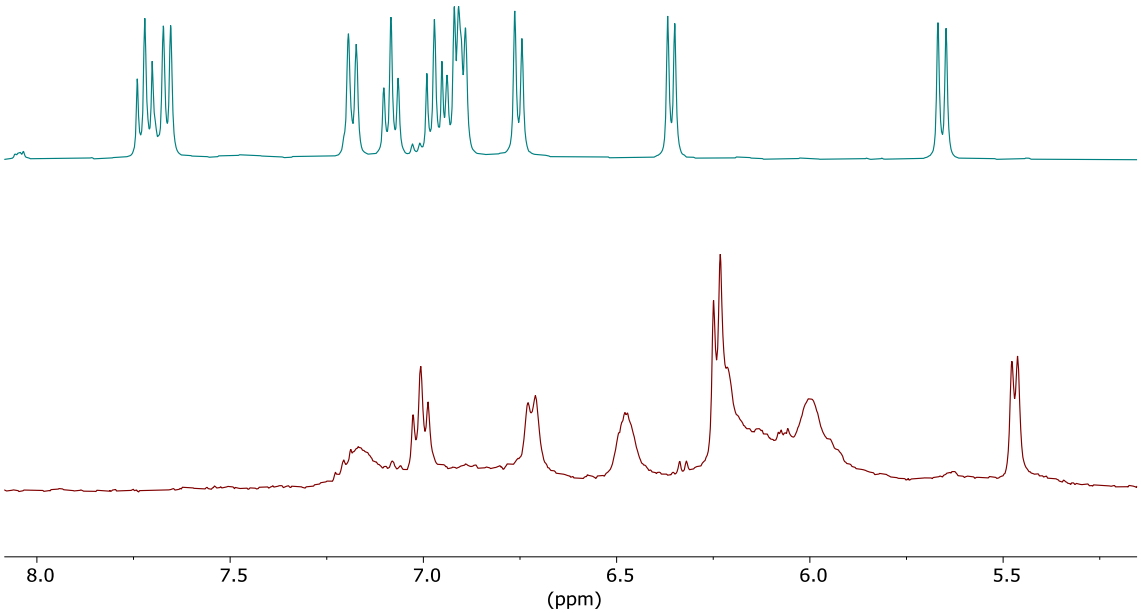

Figure S37. Aromatic region of ^{1}H NMR spectra of complexes **4-Me** (above) and **5-Me** (below).

EXchange SpectroscopY (EXSY) NMR experiments

EXSY experiments were carried out from 278 K to 303 K in toluene-d_8 to calculate the activation parameters for the conformational exchange in **1-Et**. These experiments were acquired in a Bruker-Neo 400MHz spectrometer, equipped with a Bruker BCU-II temperature control system, and using standard pulse sequences.

For each temperature, two ^{1}H 2D-NOESY spectra (pulse program *noesygpph*) were acquired on a sample of **1-Et**, with the relaxation delay d1 set to 2 s. The mixing time, d8, was set to 400 ms for the first experiment, and to ~ 0 ms for the second experiment, which was used as reference.

The experiments were processed using the TOPSPIN software by Bruker, with a π/2 sine-type window function in the F1 and F2 domains, and the areas of the diagonal and off-diagonal peaks of the hydrogens py-C*H*$_2$CH$_3$ and py'-C*H*$_2$CH$_3$ were integrated (**Figure S38**).

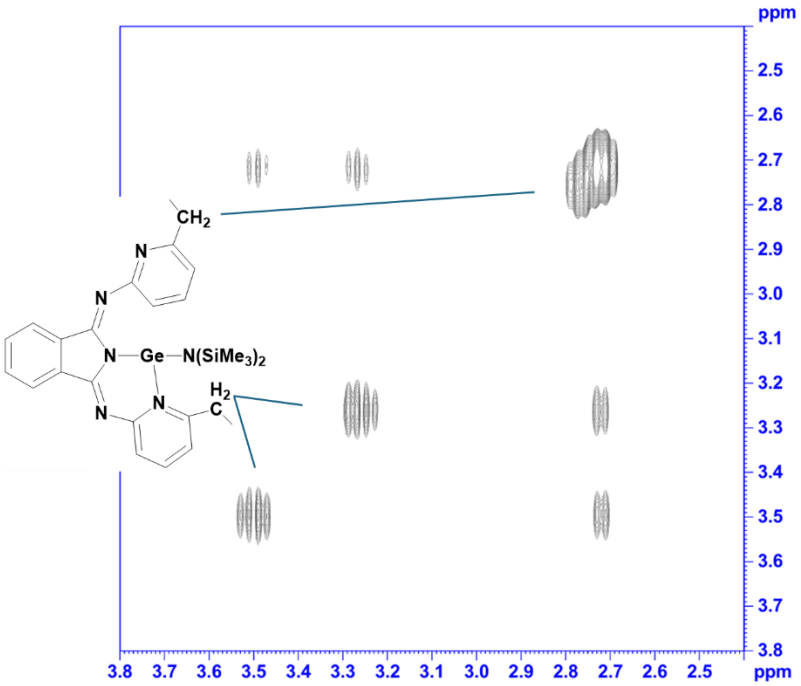

Figure S38. Methylene region of one of the 2D-NOESY spectra (303 K, d8 = 0.4s) used to study the conformational exchange of **1-Et**, showing cross-peaks between the py-C*H*$_2$CH$_3$ and py'-C*H*$_2$CH$_3$ resonances.

The rate constants for the forward and reverse exchange processes, k_1 and k_{-1}, were obtained from the integrated areas using the EXSYcalc program.[23] The activation parameters were obtained by fitting the experimental data (**Figure S40** and **Table S04**)

to the linear form of the Eyring-Polanyi equation (4), where k is the average of the rate constants k_1 and k_{-1}, T is the absolute temperature, R is the gas constant, κ is the transmission coefficient taken as 1, and h is the Plank constant.

$$(4) \quad ln\frac{k}{T} = \frac{-\Delta H^{\ddagger}}{R} \cdot \frac{1}{T} + ln\frac{\kappa k_B}{h} + \frac{\Delta S^{\ddagger}}{R}$$

Table S04. Values of magnetisation exchange rate at different temperatures obtained from 2D-EXSY experiments.

T(K)	**exchange rate** (s-1)	**1/T**	**ln(k/T)**
278.15	1.485	0.003595	-5.233
283.15	2.692	0.003532	-4.655
288.15	4.807	0.00347	-4.093
293.15	8.433	0.003411	-3.548
298.15	14.870	0.003354	-2.998
303.15	20.900	0.003299	-2.674

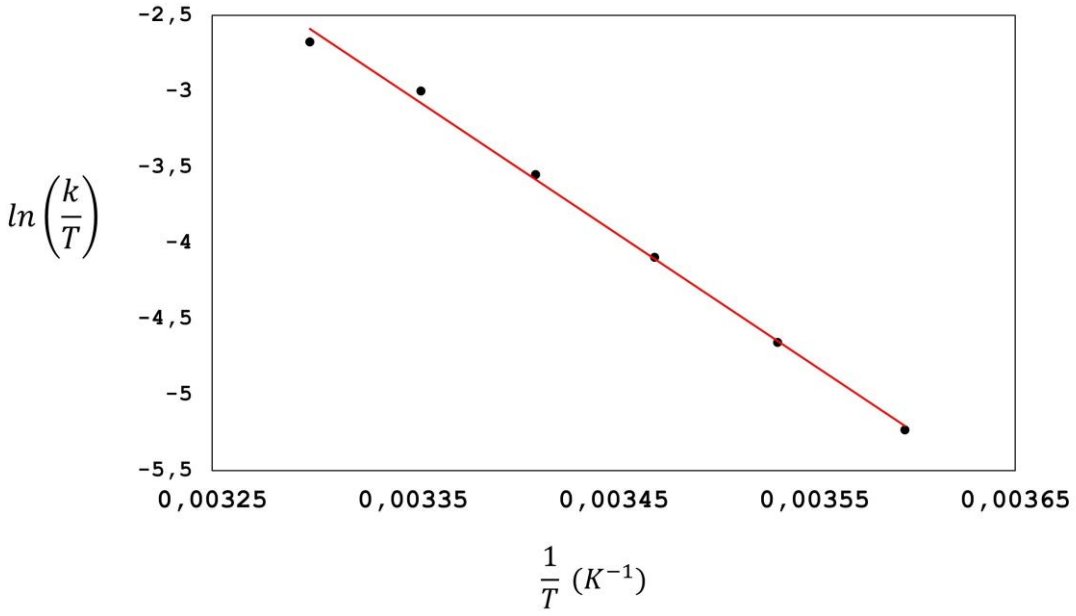

Figure S40. Eyring Plot assembled from the values of magnetisation exchange rate at different temperatures

Regression analysis of the above data yielded activation parameters: $\Delta H^{\ddagger}$ = 17 ± 2 kcal·mol^{-1}, $\Delta S^{\ddagger}$ = 5 ± 8 cal·mol^{-1}·K^{-1}, and $\Delta G_{300K}^{\ddagger}$ = 16 ± 1 kcal·mol^{-1} (errors were

estimated from the 95% confidence interval of the slope and intercept of the linear regression; $r^2 = 0.9927$)

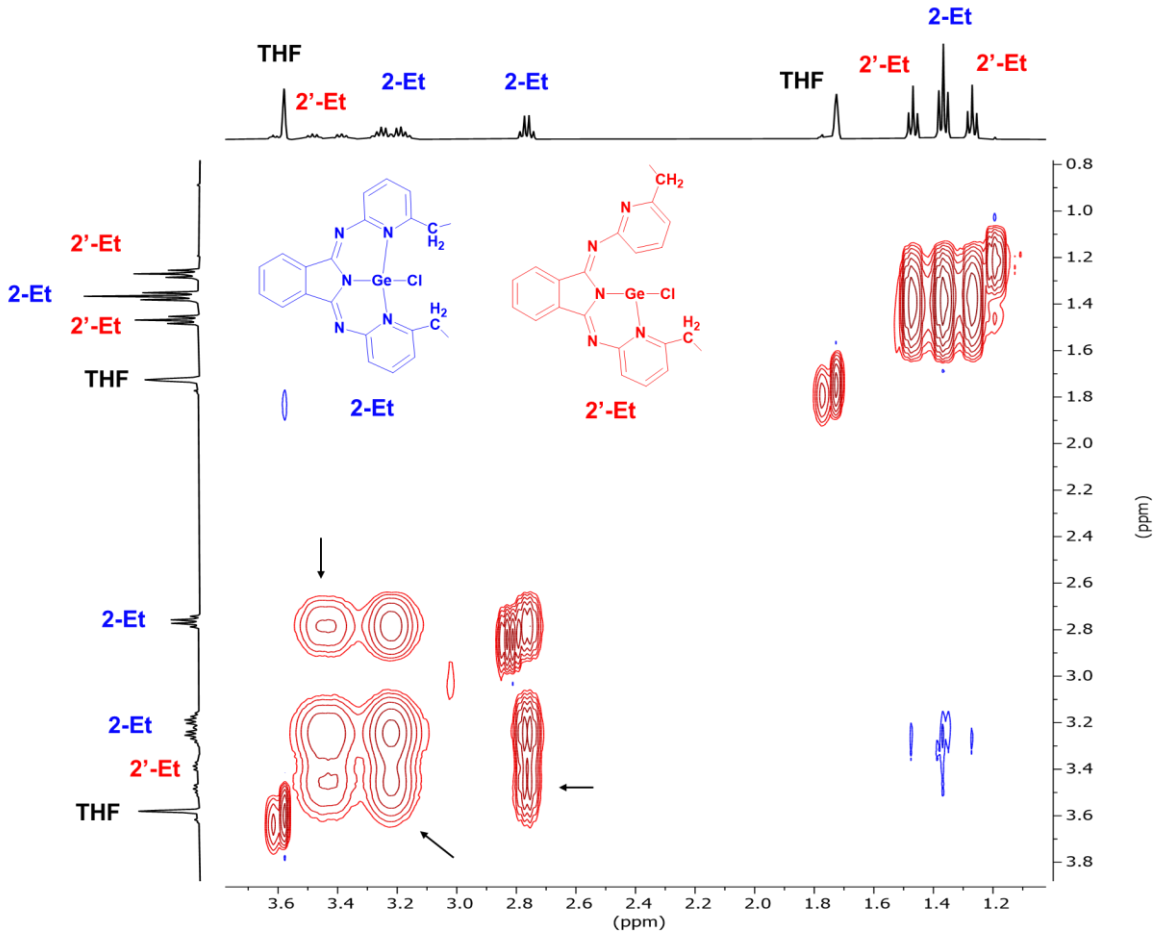

Figure S41. Methylene region of one of the 2D-EXSY spectrum (25 ºC, d8 = 1s) used to study the conformational exchange between the two isomers of **2-Et**, showing cross-peaks between the py-C*H*$_2$CH$_3$ and py'-C*H*$_2$CH$_3$ resonances.

Diffusion Ordered SpectroscopY (DOSY) NMR experiments

DOSY experiments were carried out in tetrahydrofuran-d$_8$ to calculate the diffusion coefficient for compounds **2-Me**, **4-Et** and **5-Et**. These experiments were acquired in a Bruker-Neo 400MHz spectrometer and using standard pulse sequences. Hydrodynamic radii were calculated from the values of the diffusion coefficient using the Stokes-Einstein equation (5):

$$(5) \qquad D = \frac{k_B T}{6\pi\eta r}$$

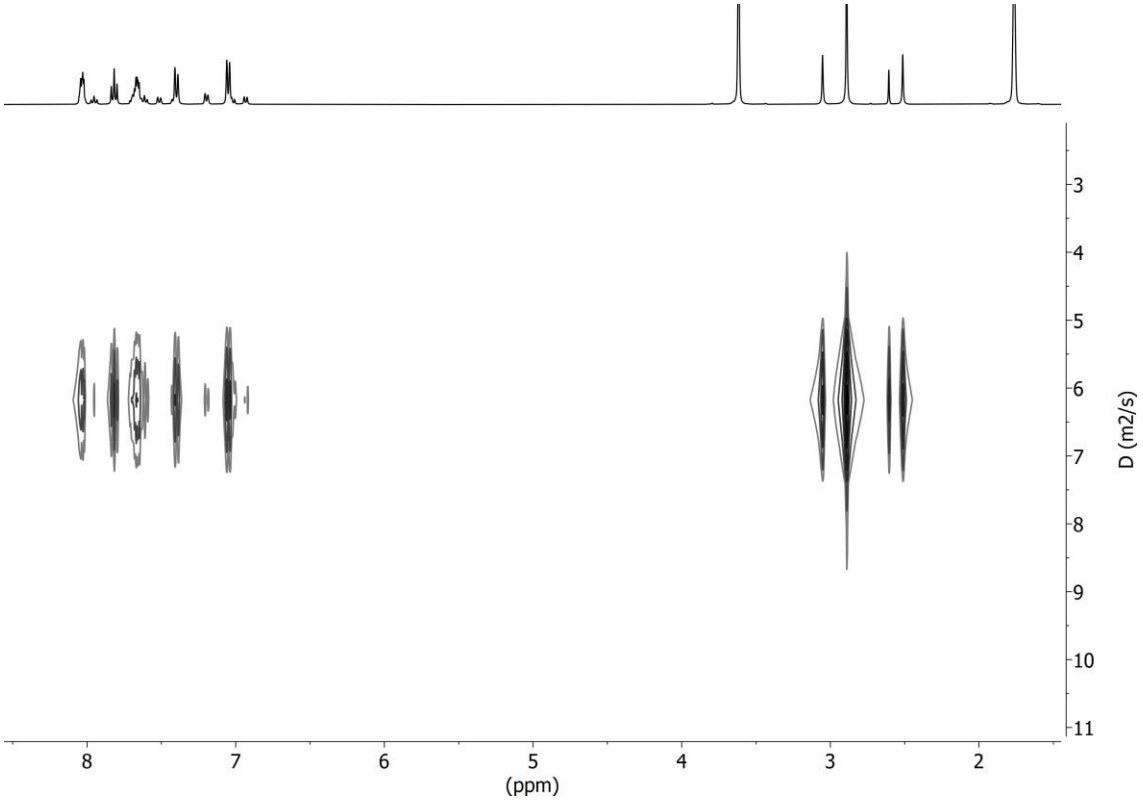

Figure S42. DOSY experiment (400 MHz, THF-d_8, 25 °C) of complex **2-Me**.

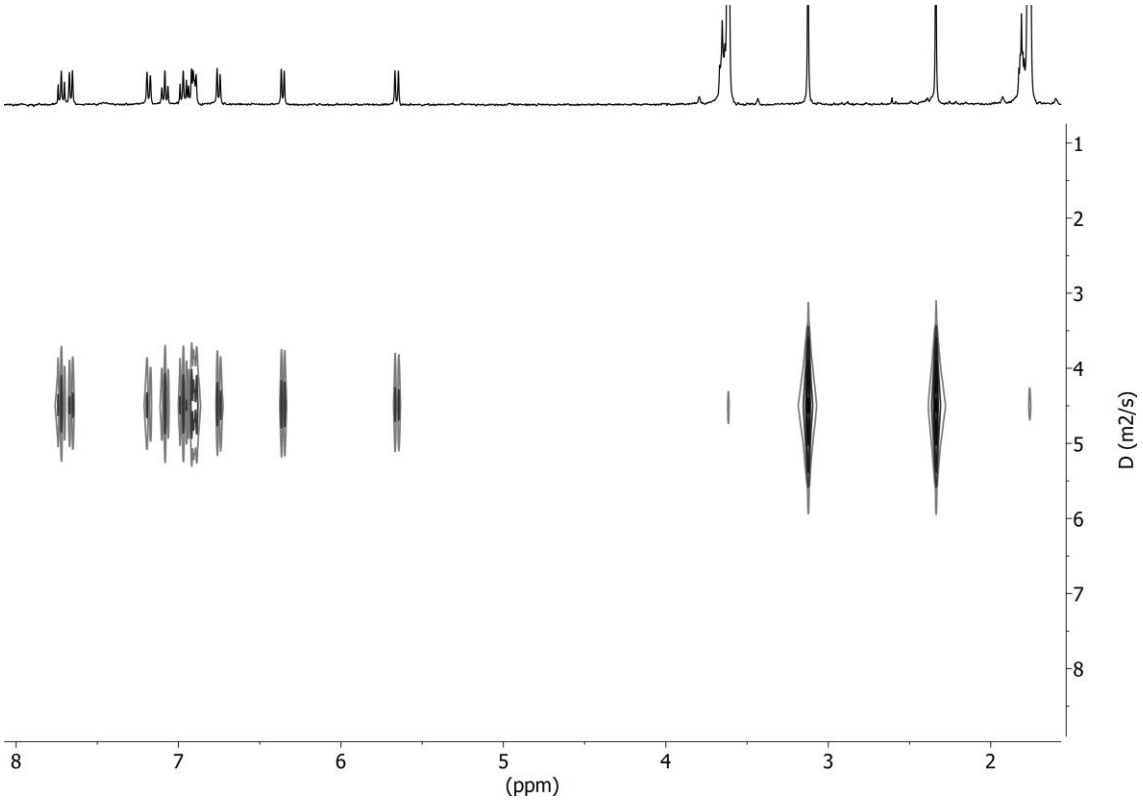

Figure S43. DOSY experiment (400 MHz, THF-d_8, 25 °C) of complex **4-Me**.

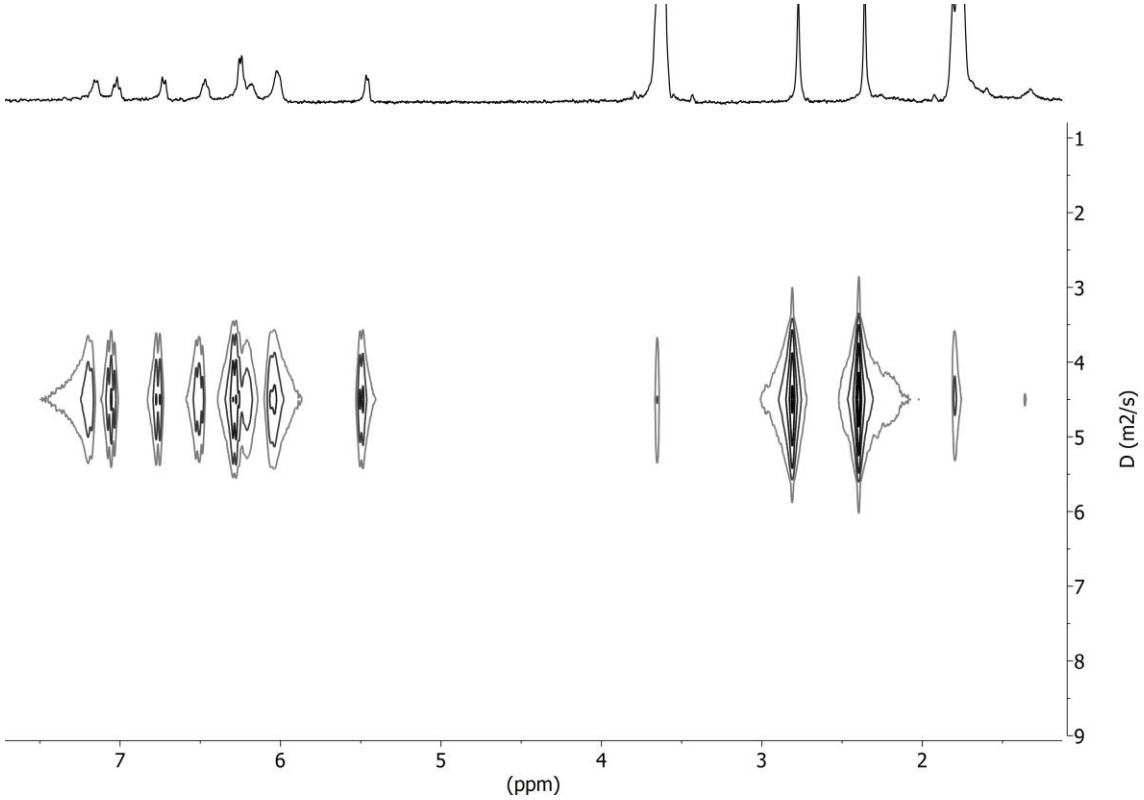

Figure S44. DOSY experiment (400 MHz, THF-d_8, 25 °C) of complex **5-Me**.

References

1 G. R. Fulmer, A. J. M. Miller, N. H. Sherden, H. E. Gottlieb, A. Nudelman, B. M. Stoltz, J. E. Bercaw and K. I. Goldberg, *Organometallics*, 2010, **29**, 2176–2179.

2 M. J. S. Gynane, D. H. Harris, M. F. Lappert, P. P. Power, P. Rivière and M. Rivière-Baudet, *J. Chem. Soc., Dalt. Trans.*, 1977, 2004–2009.

3 B. K. Langlotz, J. L. Fillol, J. H. Gross, H. Wadepohl and L. H. Gade, *Chem. - A Eur. J.*, 2008, **14**, 10267–10279.

4 D. L. J. Broere, B. Q. Mercado, E. Bill, K. M. Lancaster, S. Sproules and P. L. Holland, *Inorg. Chem.*, 2018, **57**, 9580–9591.

5 G. M. A. Sheldrick, A Short History of SHELX, *Acta Cryst*, 2008, **A64**, 112

6 Gaussian 16, Revision C.01, M. J. Frisch, G. W. Trucks, H. B. Schlegel, G. E. Scuseria, M. A. Robb, J. R. Cheeseman, G. Scalmani, V. Barone, G. A. Petersson, H. Nakatsuji, X. Li, M. Caricato, A. V. Marenich, J. Bloino, B. G. Janesko, R. Gomperts, B. Mennucci, H. P. Hratchian, J. V. Ortiz, A. F. Izmaylov, J. L. Sonnenberg, D. Williams-Young, F. Ding, F. Lipparini, F. Egidi, J. Goings, B. Peng, A. Petrone, T. Henderson, D. Ranasinghe, V. G. Zakrzewski, J. Gao, N. Rega, G. Zheng, W. Liang, M. Hada, M. Ehara, K. Toyota, R. Fukuda, J. Hasegawa, M. Ishida, T. Nakajima, Y. Honda, O. Kitao, H. Nakai, T. Vreven, K. Throssell, J. A. Montgomery, Jr., J. E. Peralta, F. Ogliaro, M. J. Bearpark, J. J. Heyd, E. N. Brothers, K. N. Kudin, V. N. Staroverov, T. A. Keith, R. Kobayashi, J. Normand, K. Raghavachari, A. P. Rendell, J. C. Burant, S. S. Iyengar, J. Tomasi, M. Cossi, J. M. Millam, M. Klene, C. Adamo, R. Cammi, J. W. Ochterski, R. L. Martin, K. Morokuma, O. Farkas, J. B. Foresman, and D. J. Fox, Gaussian, Inc., Wallingford CT, 2019.

7 A. D. Becke, *J. Chem. Phys.*, 1993, **98**, 5648–5652.

8 C. Lee, W. Yang and R. G. Parr, *Phys. Rev. B*, 1988, **37**, 785–789.

9 R. Ditchfield, W. J. Hehre and J. A. Pople, *J. Chem. Phys.*, 1971, **54**, 724–728.

10 W. J. Hehre, R. Ditchfield and J. A. Pople, *J. Chem. Phys.*, 1972, **56**, 2257–2261.

11 P. C. Hariharan and J. A. Pople, *Theor. Chim. Acta*, 1973, **28**, 213–222.

12 M. S. Gordon, J. S. Binkley, J. A. Pople, W. J. Pietro and W. J. Hehre, *J. Am. Chem. Soc.*, 1982, **104**, 2797–2803.

13 M. M. Francl, W. J. Pietro, W. J. Hehre, J. S. Binkley, M. S. Gordon, D. J. DeFrees and J. A. Pople, *J. Chem. Phys.*, 1982, **77**, 3654–3665.

14 V. A. Rassolov, M. A. Ratner, J. A. Pople, P. C. Redfern and L. A. Curtiss, *J. Comput. Chem.*, 2001, **22**, 976–984.

15 S. Grimme, J. Antony, S. Ehrlich and H. Krieg, *J. Chem. Phys.*, , DOI:10.1063/1.3382344.

16 S. Grimme, S. Ehrlich and L. Goerigk, *J. Comput. Chem.*, 2011, **32**, 1456–1465.

17 A. V. Marenich, C. J. Cramer and D. G. Truhlar, *J. Phys. Chem. B*, 2009, **113**, 6378–6396.

18 L. E. Roy, E. Jakubikova, M. G. Guthrie and E. R. Batista, *J. Phys. Chem. A*, 2009, **113**, 6745–6750.

19 J. O. Wenzel, I. Fernández and F. Breher, *Eur. J. Inorg. Chem.*, 2023, **26**, e202300315.

20 a) Multiwfn - A Multifunctional Wavefunction Analyzer Version 3.8(dev), release date: 2023-Aug-12, Developer: Tian Lu; b) T. Lu and F. Chen, *J. Comput. Chem.*, 2012, **33**, 580–592.

21 G. A. Zhurko, Chemcraft, version 1.8 (build 688b) - graphical program for visualization of quantum chemistry computations. Ivanovo, Russia, 2005. https://chemcraftprog.com.

22 E. D. Glendening, C. R. Landis and F. Weinhold, *J. Comput. Chem.*, 2013, **34**, 1429–1437.

23 J. C. Cobas and M. Martín-Pastor, EXSYCalc, version 1.0. MestreLab. https://mestrelab.com/software/freeware/.